Introduction to gamma-ray blazars

Deirdre HORAN
LLR / Ecole Polytechnique
deirdre@llr.in2p3.fr

OUTLINE

1. Active galactic nuclei
2. Blazars
3. Models of blazar emission
4. The Fermi blazars
5. The TeV blazars
6. The GeV-TeV Connection
7. The extra-galactic background light
8. Intergalactic magnetic fields
9. Characterising variability

Active galactic nuclei
- 1/9 -

Active Galactic Nuclei

CHARACTERISTICS

- central nucleus outshines the rest of the galaxy
- high luminosity (normally)
- emission across entire spectrum ... radio to keV, MeV, TeV
  - ➡ non-thermal
- strong variability
- radio-loud sources:
  - ➡ relativistic jets ... superluminal motion

Active Galactic Nuclei

TAXONOMY

Active Galactic Nuclei

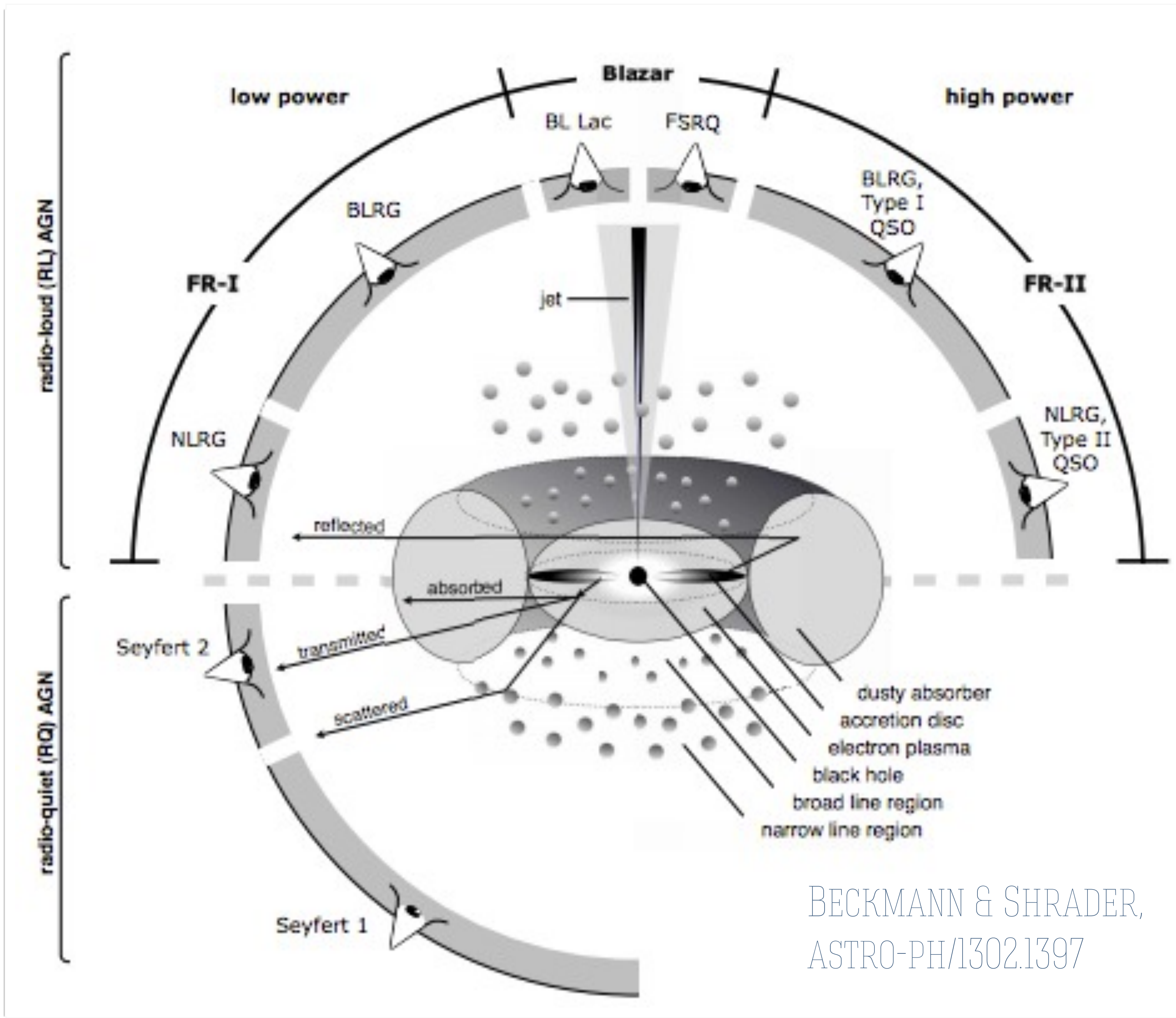

Beckmann & Shrader, astro-ph/1302.1397

Active Galactic Nuclei CLASSIFICATION

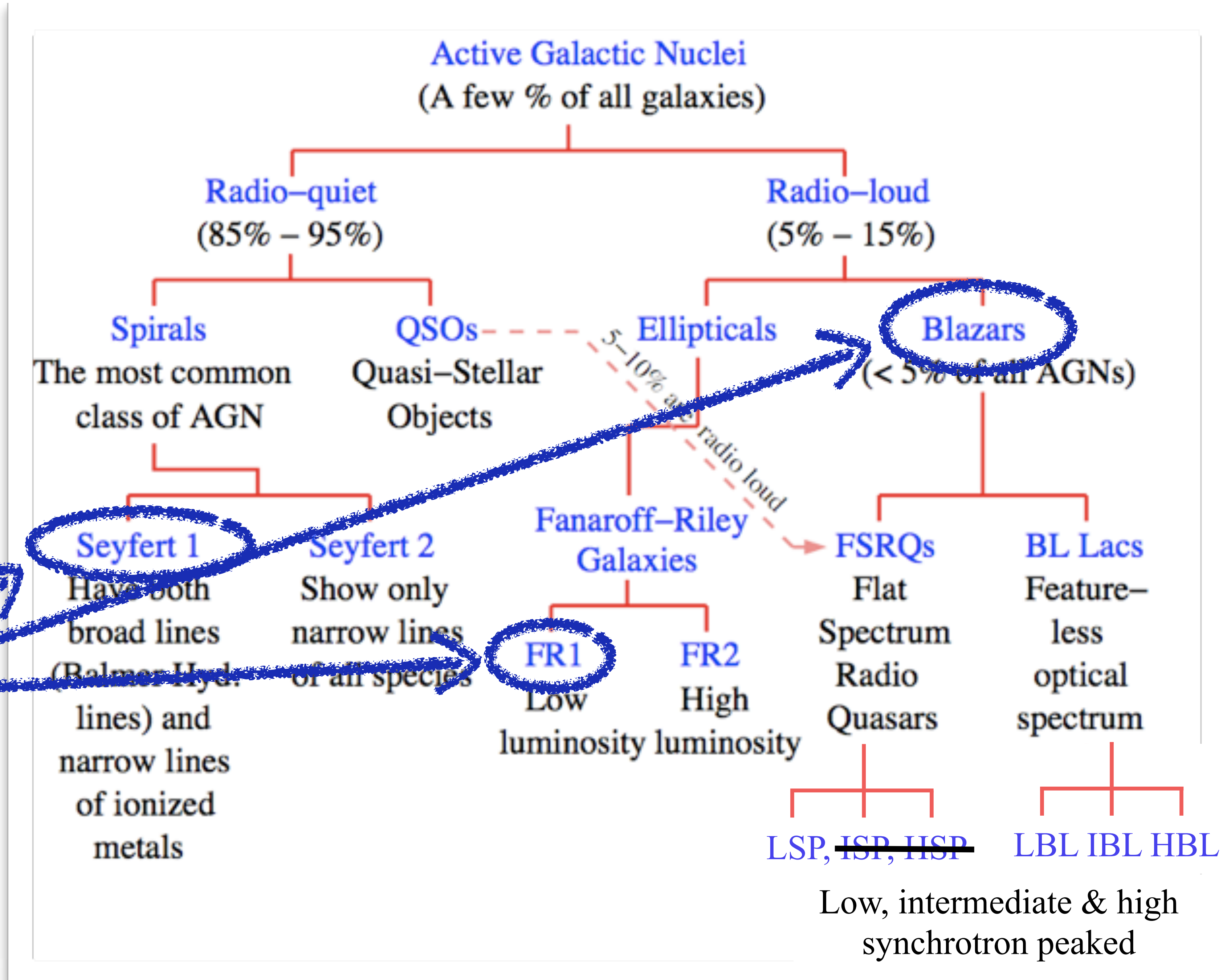

identified as Fermi sources

Active Galactic Nuclei

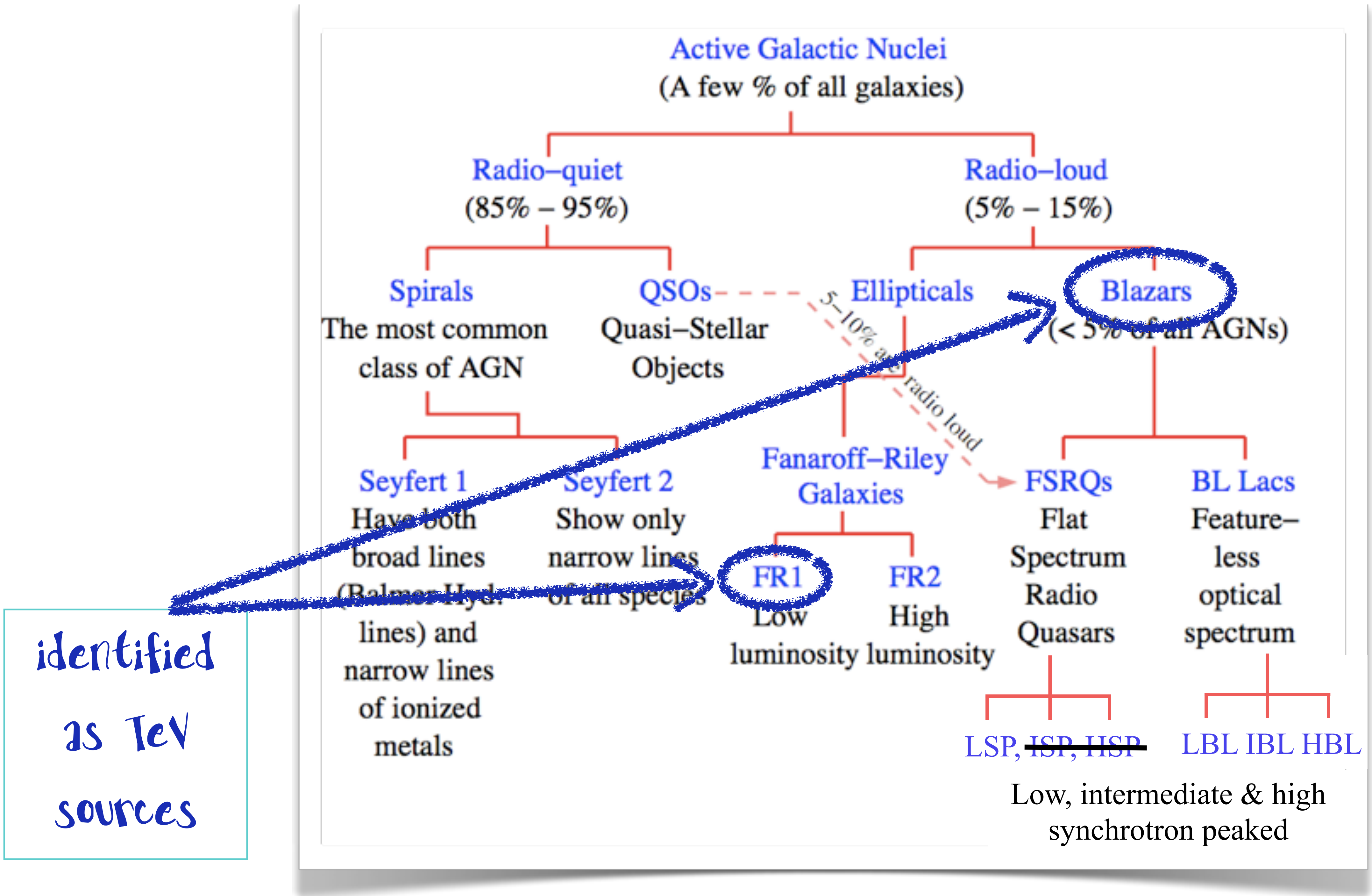

Blazars

2/9

Blazars

CHARACTERISTICS

- <5% of all AGN
- jet points "at" us
- flat radio spectrum
- **radio loud AGN**
- large amplitude variability
- **optical polarisation**
- spectral energy distribution

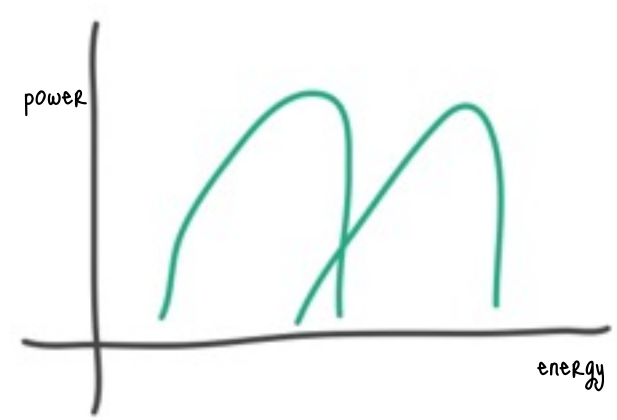

Blazars

Superluminal motion

First proposed by Rees in 1966 (Nature, 211, 468) years before it was first observed when VLBI techniques were developed

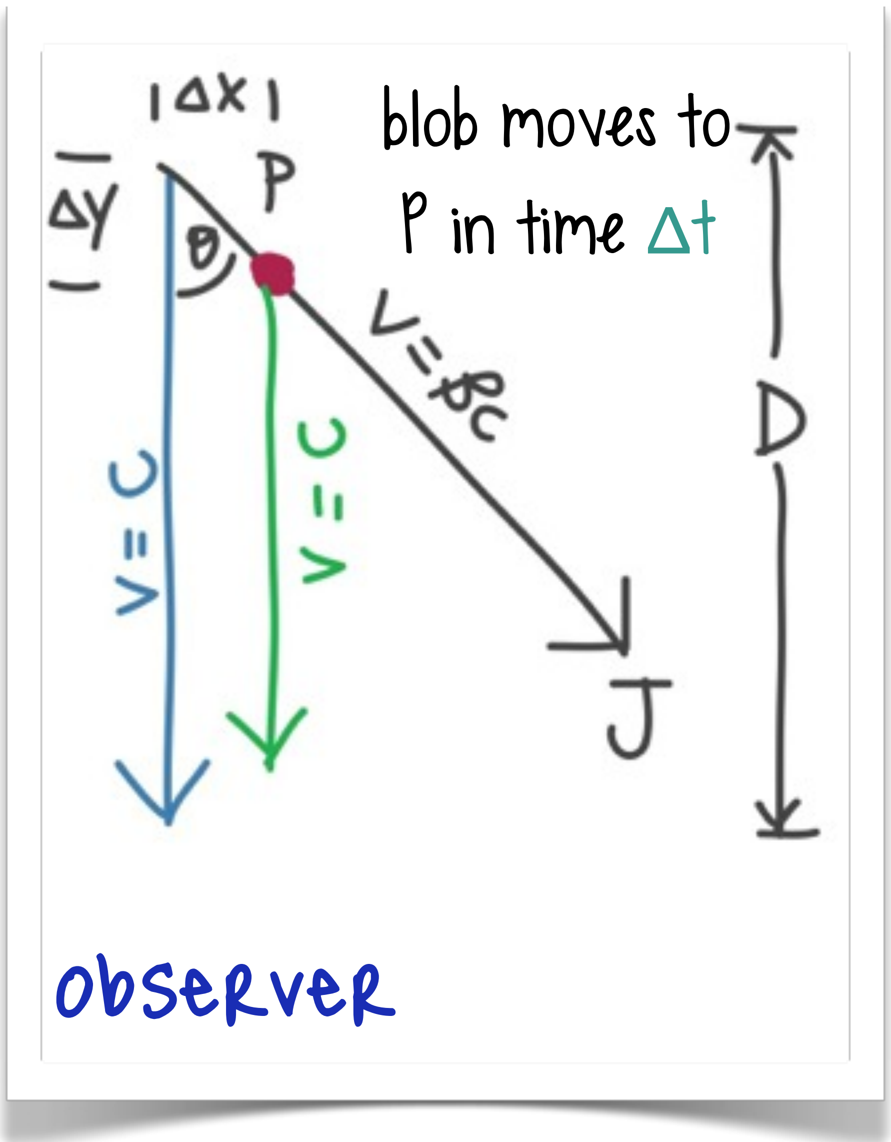

first pulse travels to observer in time D/c; the second, emitted time Δt later, has a shorter distance to travel: D-Δy.

Difference in arrival time is:

$$\Delta t_{obs} = \left[\Delta t + \frac{(D-\Delta y)}{c}\right] - \left[\frac{D}{c}\right]$$

Blazars

Superluminal motion

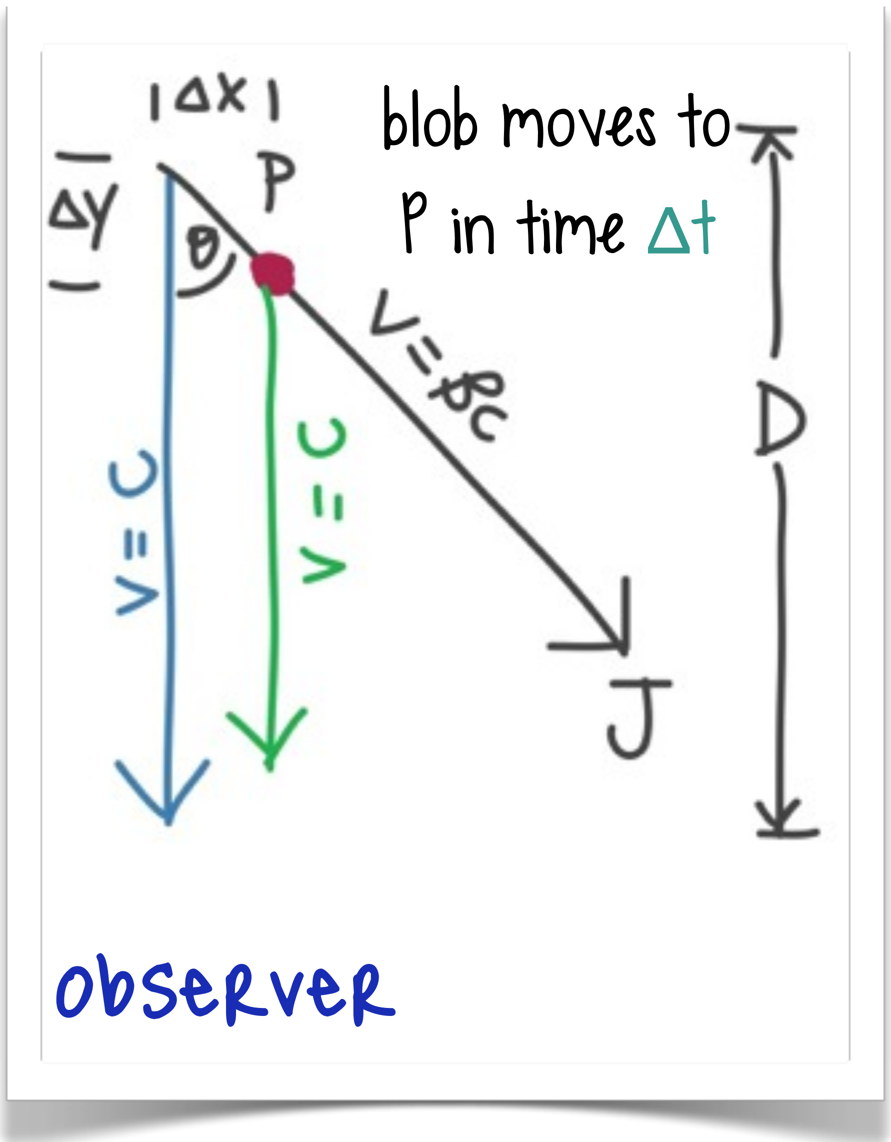

Difference in arrival time is:

$$\Delta t_{obs} = \left[\Delta t + \frac{(D - \Delta y)}{c}\right] - \left[\frac{D}{c}\right]$$

substitute for Δy & rearrange:

$$\Delta t_{obs} = \Delta t\left(1 - \beta\cos\theta\right)$$

measured transverse velocity, v_{obs}

$$v_{obs} = \frac{\Delta x}{\Delta t_{obs}} = \frac{\beta c \sin\theta}{(1 - \beta\cos\theta)}$$

therefore:

$$\beta_{obs} = \frac{\beta\sin\theta}{(1 - \beta\cos\theta)}$$

Blazars

Superluminal motion

So, if the plasma velocity was 0.95c and the angle to the observer was 5deg, the apparent velocity would be 1.5c. The effect is maximised when $\cos\theta = \beta$

$$\beta_{obs} = \frac{\beta \sin\theta}{(1 - \beta\cos\theta)}$$

Blazars

Relativistic beaming

- Another relativistic effect occurs because the knots of plasma are moving at velocities close to that of light
- When an emitting plasma has a bulk relativistic motion relative to a fixed observer, its emission is beamed in the forward direction in the fixed frame
- The flux density is thus changed by relativistic time dilation so an observer sees much more intense emission than if the plasma were at rest
- The observed emission, S_{obs} is boosted in energy over that emitted in the rest frame, S

Definitions:

The Doppler factor is a measure of the strength of the beaming: $\delta = [\Gamma(1-\beta\cos\theta)]^{-1}$

The Lorenz factor: $\Gamma = \frac{1}{\sqrt{1-\beta^2}}$ where $\beta = \frac{v}{c}$

$$S_{obs} = S[\Gamma(1-\beta\cos\theta)]^{-3}$$

If plasma velocity is 0.95c and θ is 5deg, the boosting factor will be ~198

Blazars

Pair-production optical depth

*Dondi & Ghisellini (1995) MNRAS, 273, 583
**Urry & Padovani (1995) PASP, 107, 803

- High energy gamma rays collide with softer radiation to produce e^+e^- pairs
- For gammas to escape from a source, the optical depth for this process τ_e must be sufficiently low
- The cross section for this process is maximized for collisions between gamma rays of energy ...

$$x_\gamma = \frac{h\nu_\gamma}{mc^2}$$ and target photons of energy ... $$x_{target} = \frac{1}{x_\gamma}$$

- The optical depth is then defined as: $$\tau_{e^\pm} = \frac{\sigma_T}{5} N x_{target} R$$

... where N is the number of soft photons, R is the radius of the plasma "blob" (assumed shape) and σ_T is the Thompson-scattering cross section*

- A useful parameter that can then be derived** is the compactness of the source - it is a direct measure of the importance of the pair-production process $$\ell = \frac{L}{R}\frac{\sigma_T}{m_e c^3}$$

- The criterion for gammas to escape from a source is ... $$\tau_{e^\pm} \sim \frac{\ell}{40} \ll 1$$

Blazars

SPECTRAL ENERGY DISTRIBUTION

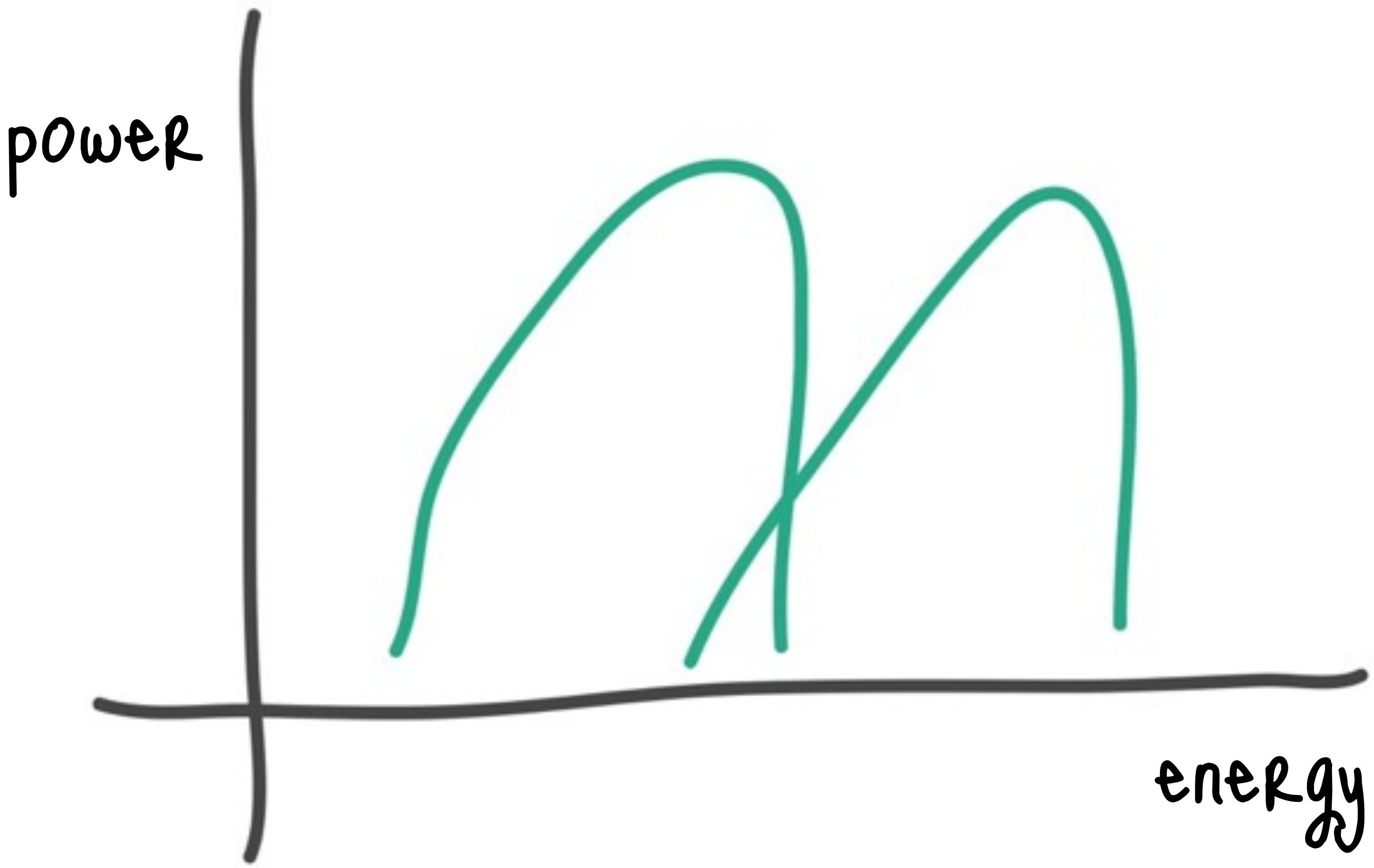

Blazars

SPECTRAL ENERGY DISTRIBUTION

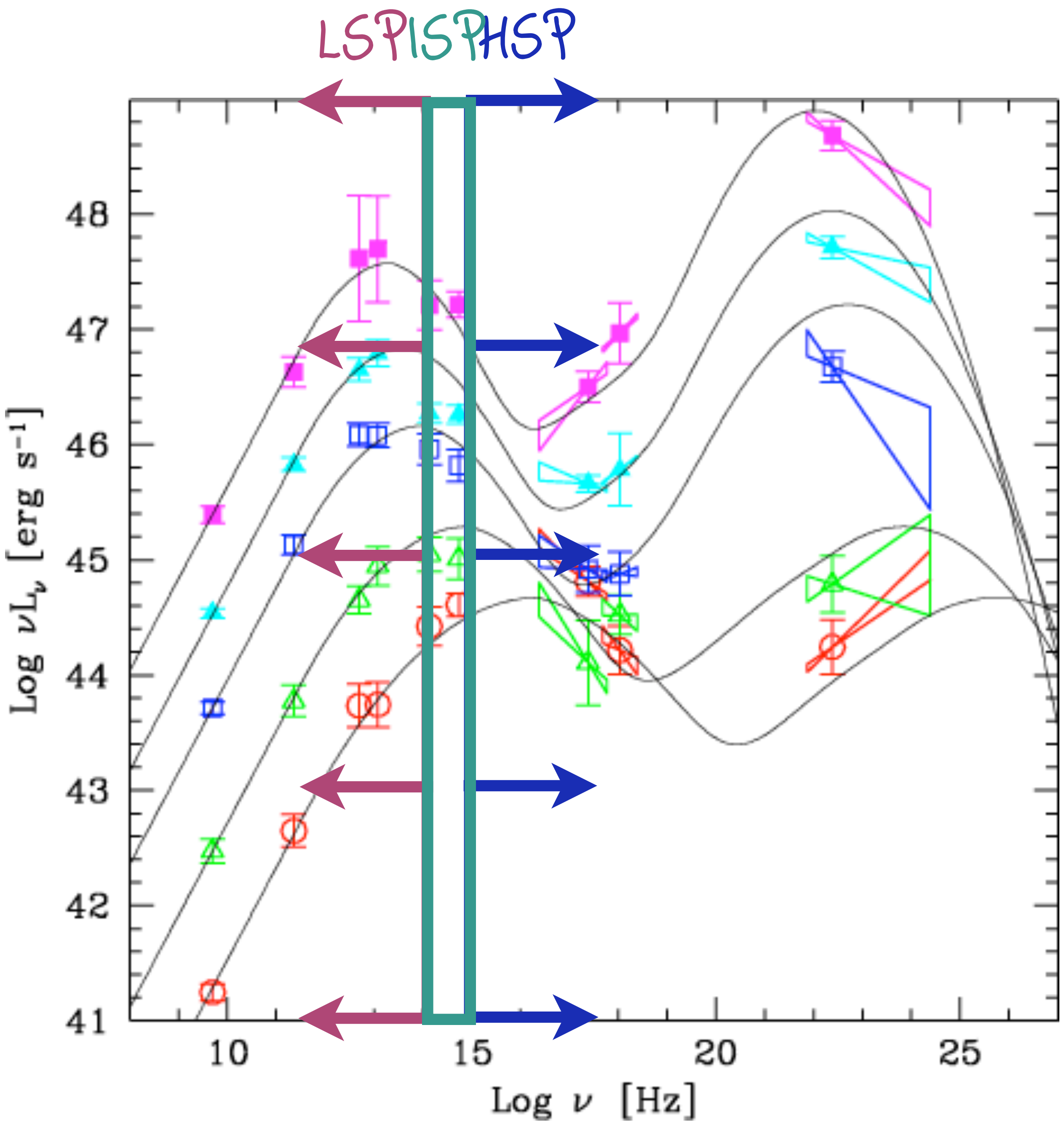

Before, definitions were based on ratio of flux at 5GHz to that at 1 keV

Models of blazar emission

3/9

Models of blazar emission

SPECTRAL ENERGY DISTRIBUTION

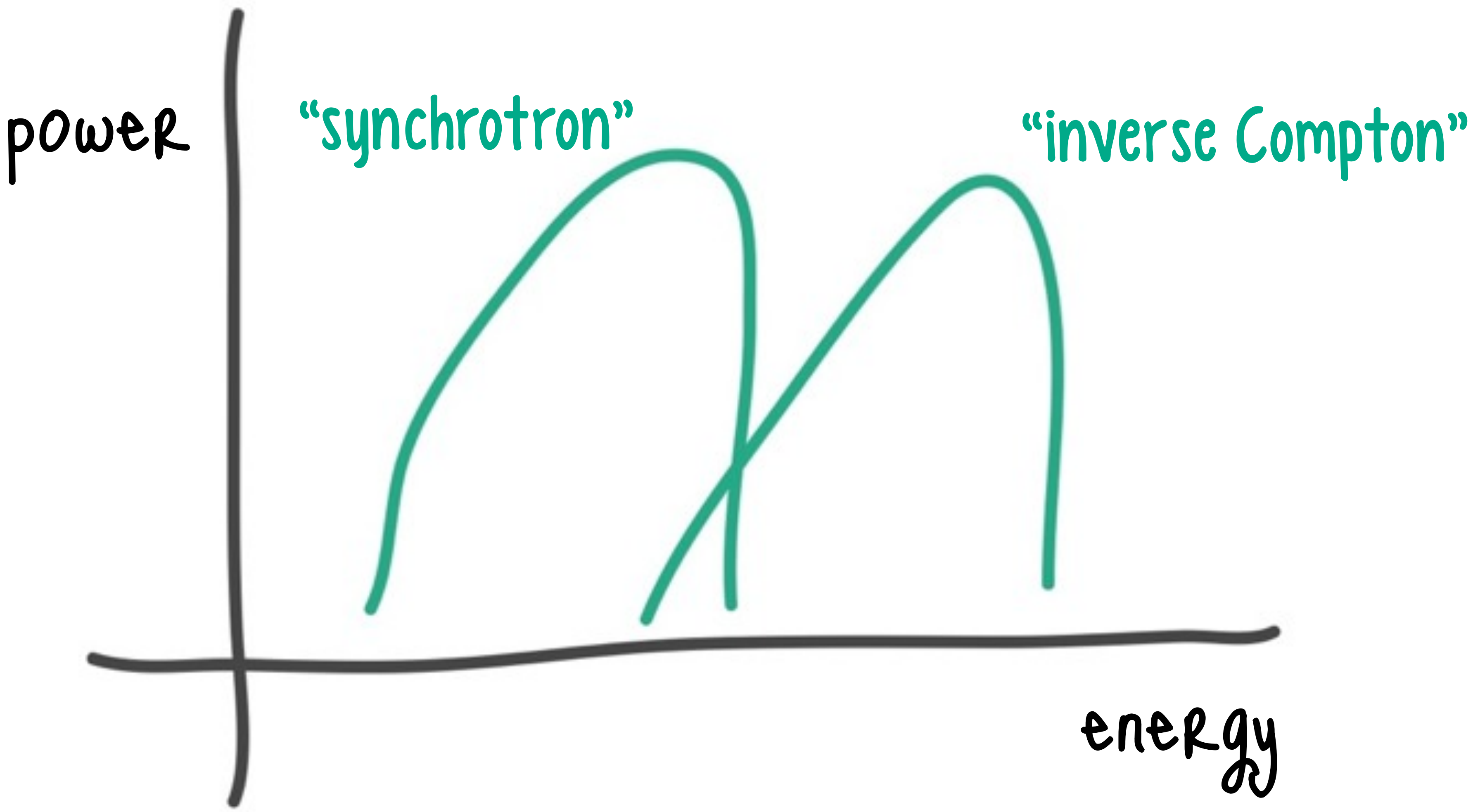

Models of blazar emission

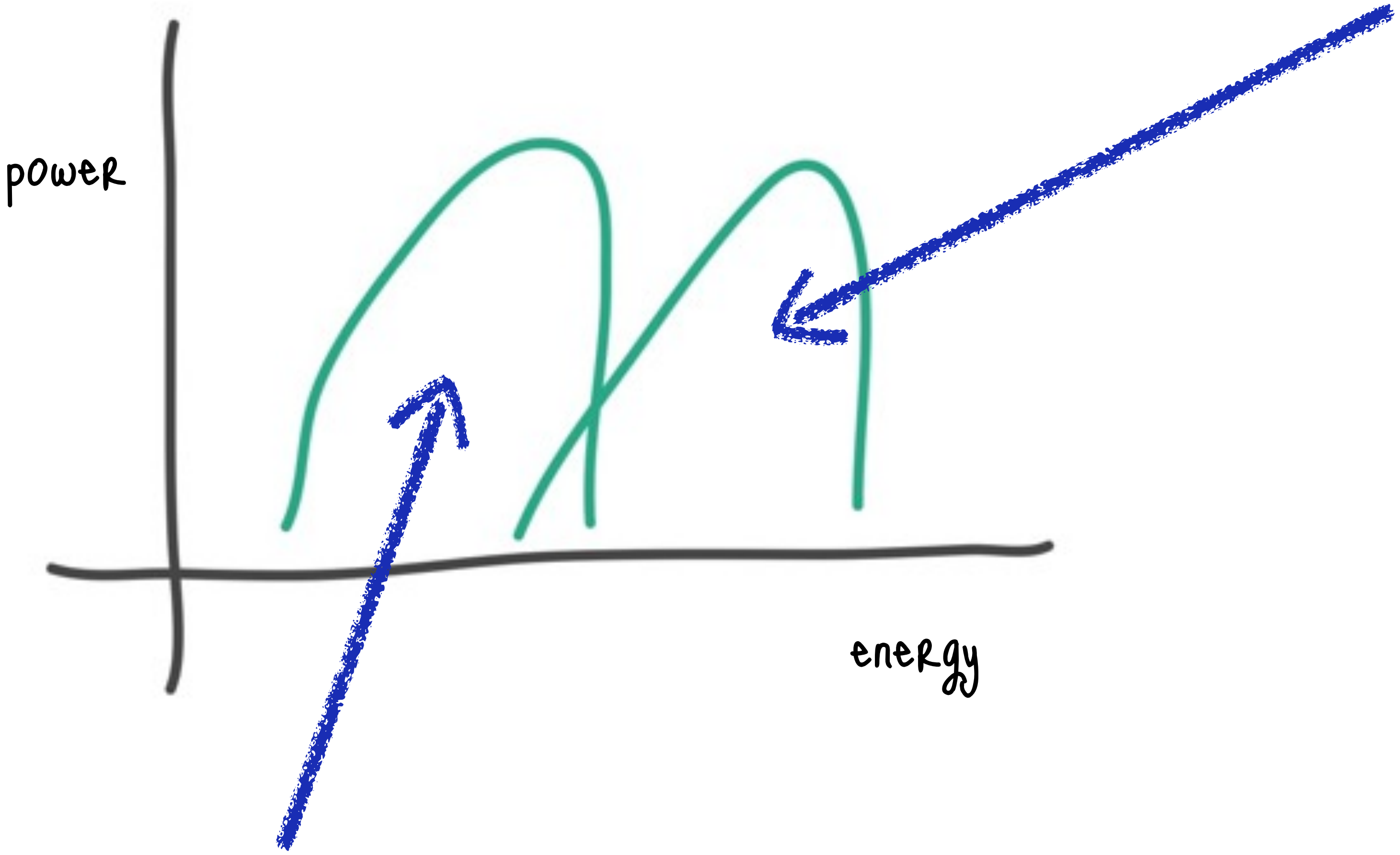

Two fundamentally different approaches to explain the higher energy emission

- Leptonic & Hadronic

Lower energy emission due to synchrotron emission from relativistic e⁻s in the jet

Models of blazar emission

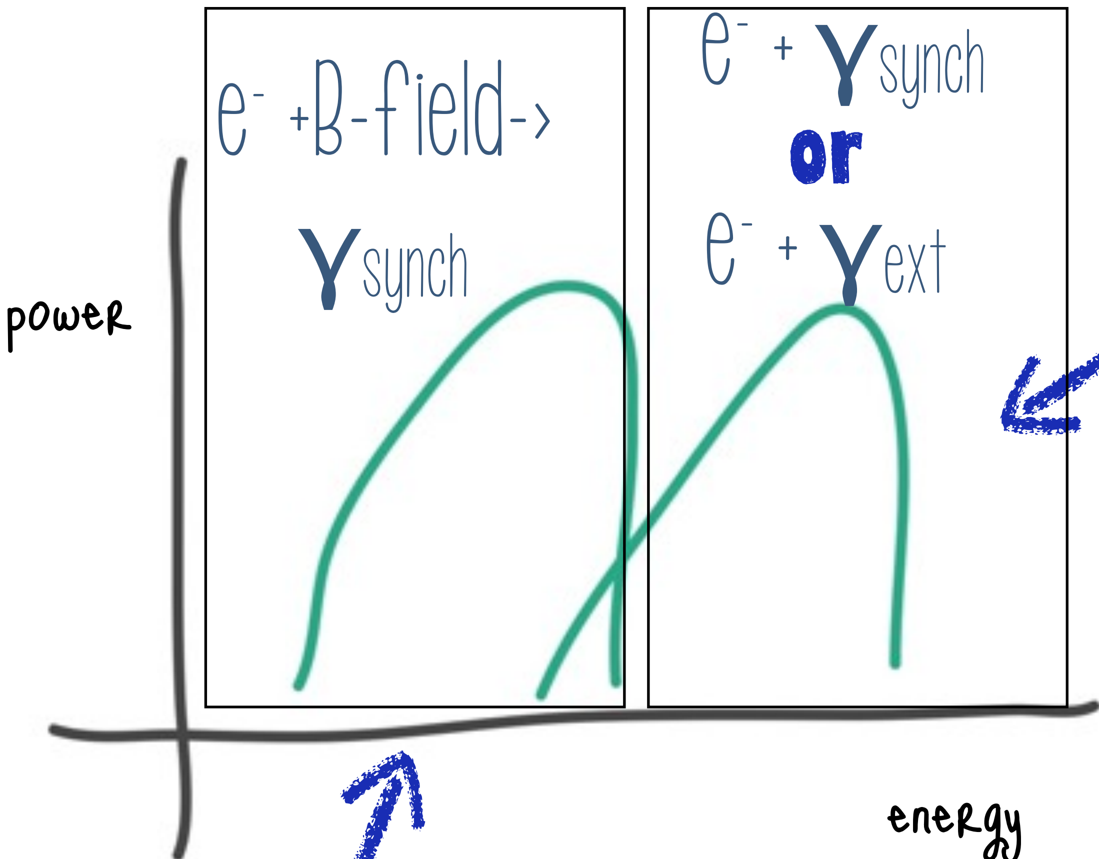

Lower energy emission due to synchrotron emission from relativistic e⁻s in the jet

Two fundamentally different approaches to explain the higher energy emission

- Leptonic & Hadronic

- radiative output dominated by e^-/e^+
- high-energy photons most likely the result of inverse Compton scattering by the same e⁻s that produced the synch
  - upscatter the low-energy photons responsible for first bump
    - ➡ synchrotron self-Compton
  - upscatter photons from the broad-line region, disc, torus ...
    - ➡ external Compton

Models of blazar emission

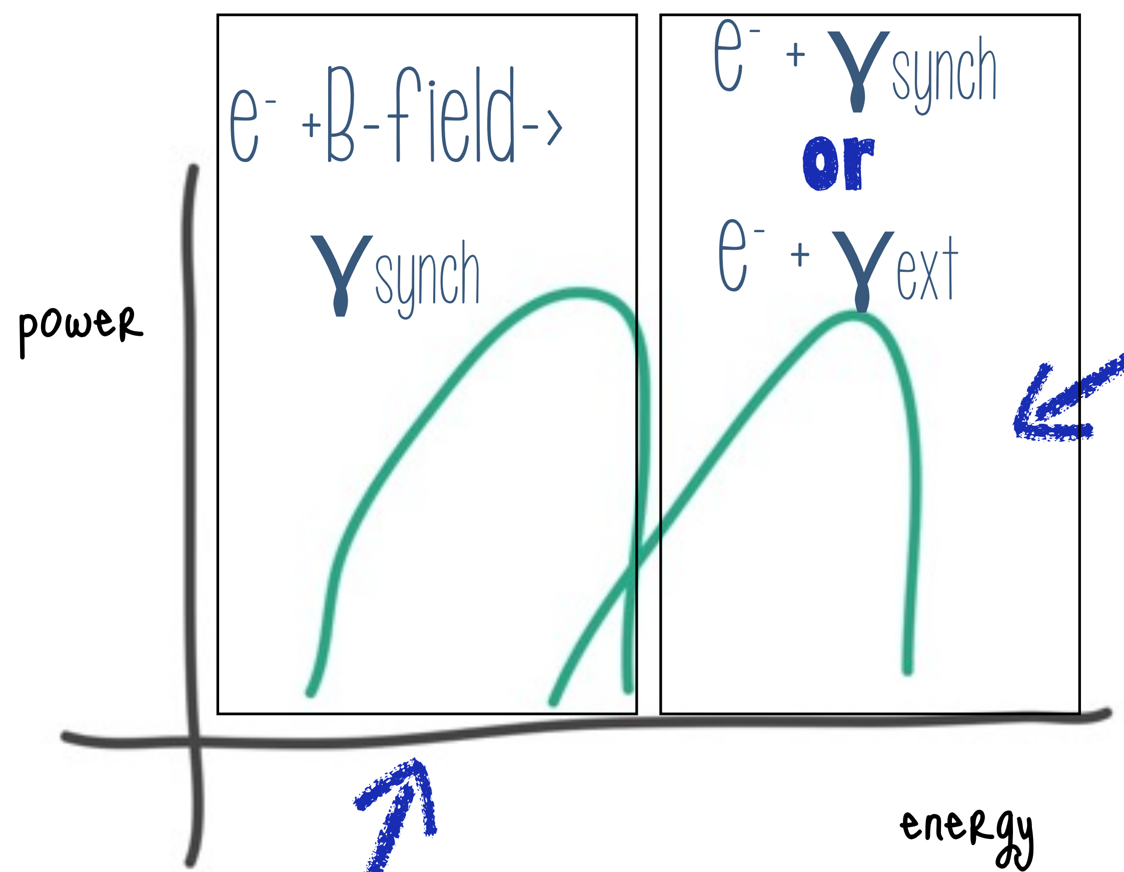

Two fundamentally different approaches to explain the higher energy emission

Leptonic & **Hadronic**

- both e^-/e^+ and p accelerated to ultra-relativistic energies
- p's exceed threshold for pγ photo-pion production on soft photon field in emission region
- high energy emission dominated by
  - ➡ proton synchrotron
  - π^0 decay products
  - synchrotron and Compton emission from secondary products of charged pions
  - ➡ external Compton

Lower energy emission due to synchrotron emission from relativistic e⁻s in the jet

Boettcher, M. (2012) Fermi & Jansky, astro-ph/1205.0539
Boettcher M. (2013), ApJ (in press), astro-ph/1304.0605

Models of blazar emission

- leptonic models provide good fits to many blazars

RBS 0413 (Aliu et al. 2012, ApJ, 750, 94)

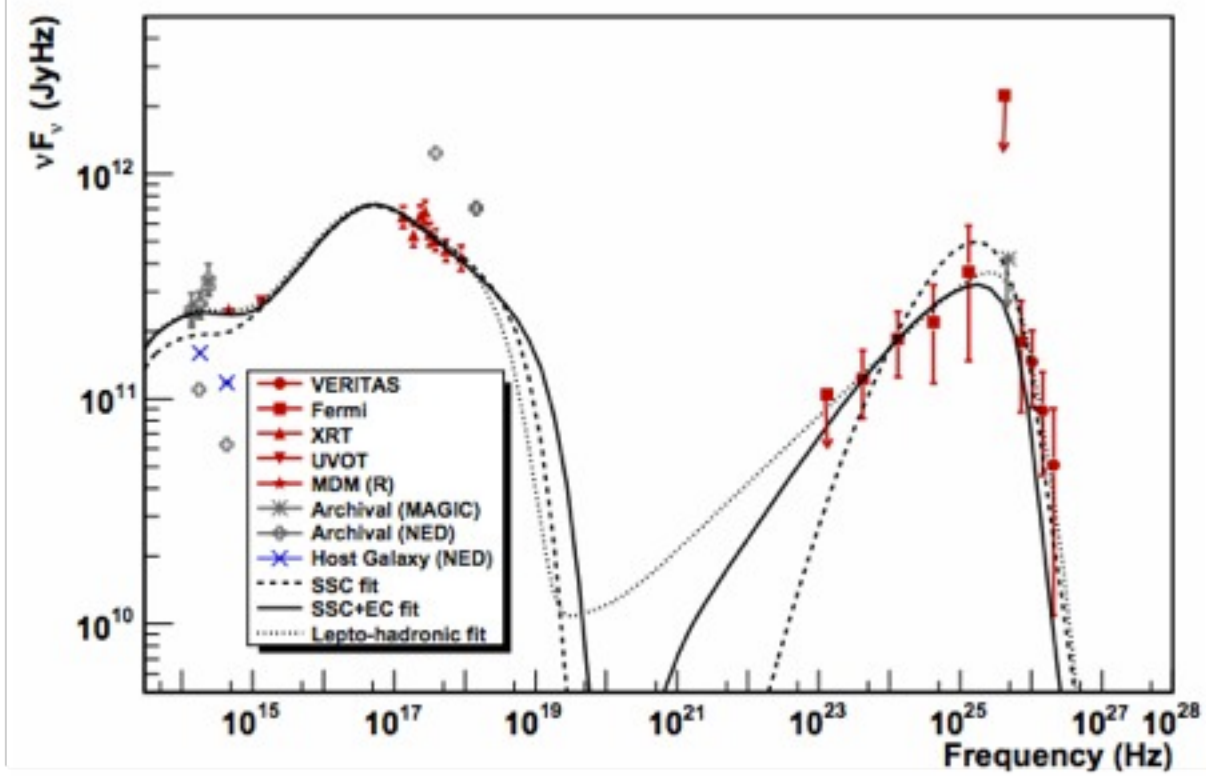

Models of blazar emission

- leptonic models provide good fits to many blazars
- **X-ray and gamma-ray emission often correlated - a fact naturally explained by SSC models**

Blazejowski, M. et al. 2005, ApJ, 630, 130

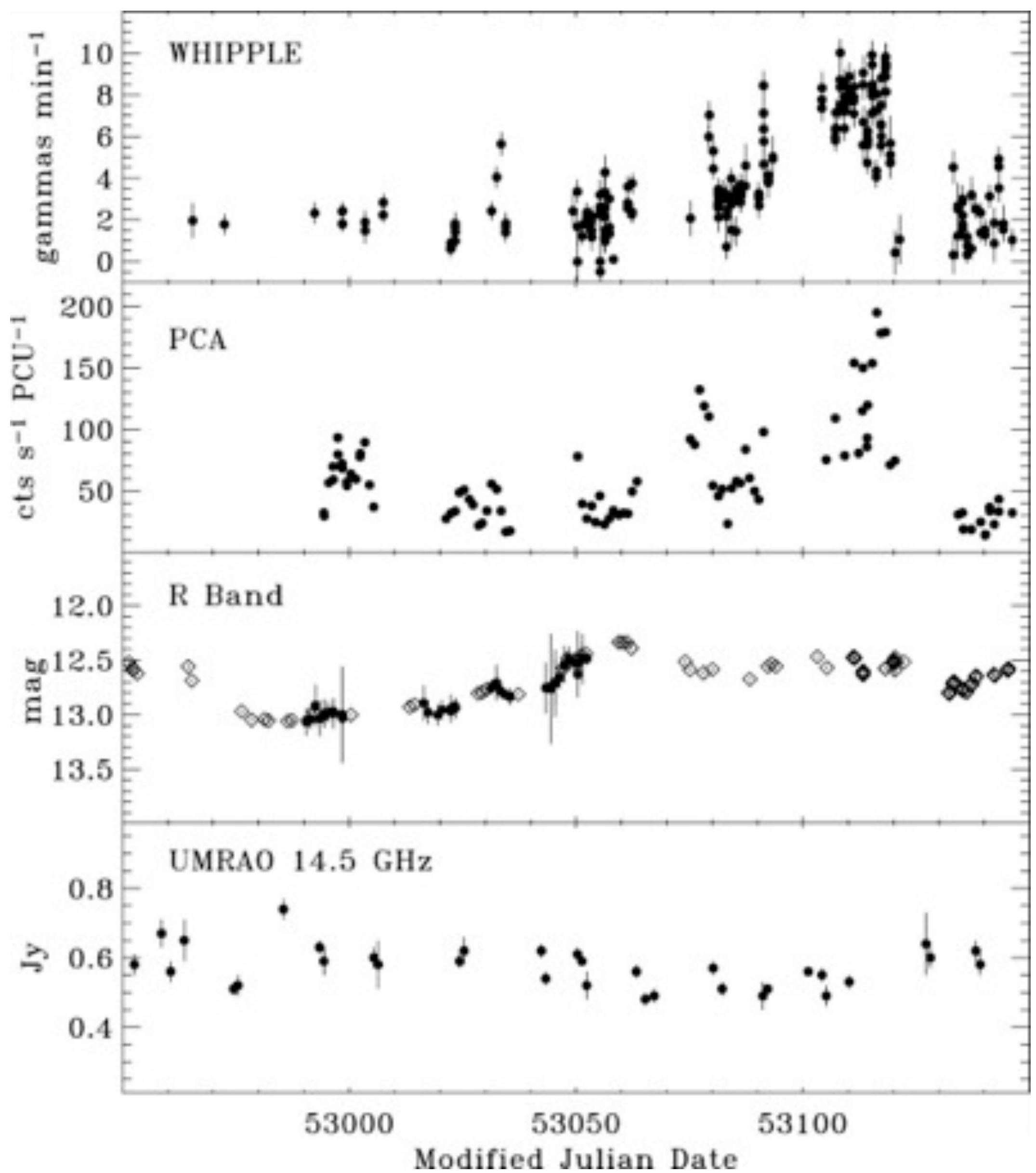

Fortson et al. (2012) Gamma 2012

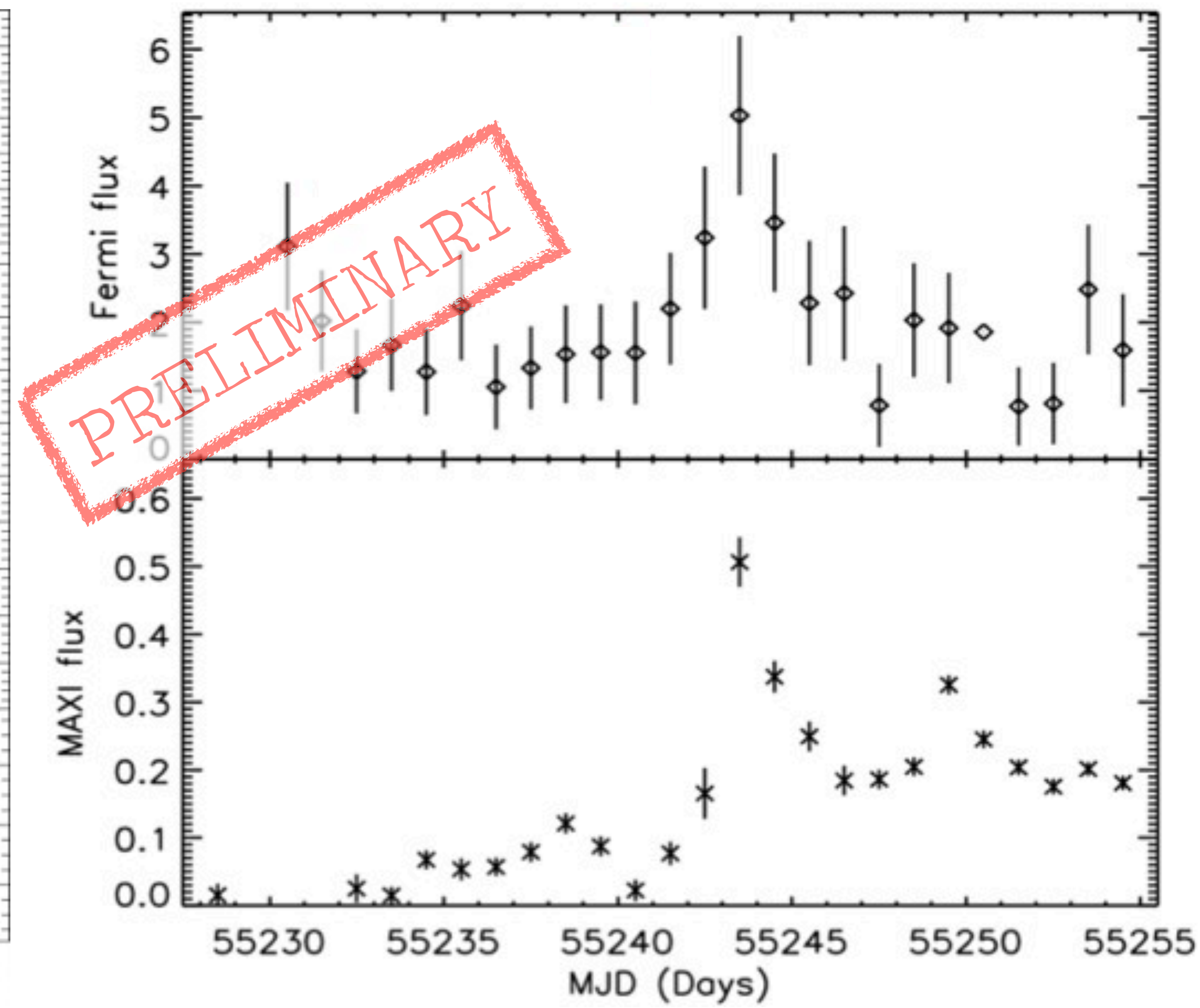

Models of blazar emission

- leptonic models provide good fits to many blazars
- **X-ray and gamma-ray emission often correlated - a fact naturally explained by SSC models**
- in hadronic models, the cooling times are longer, which makes it more difficult to explain the rapid variability often seen in blazars

➡ proton synchrotron can produce rapid variability with very high energy protons in extremely magnetised, compact regions Holder, J. (2012), Astropart. Phys., 39, 61

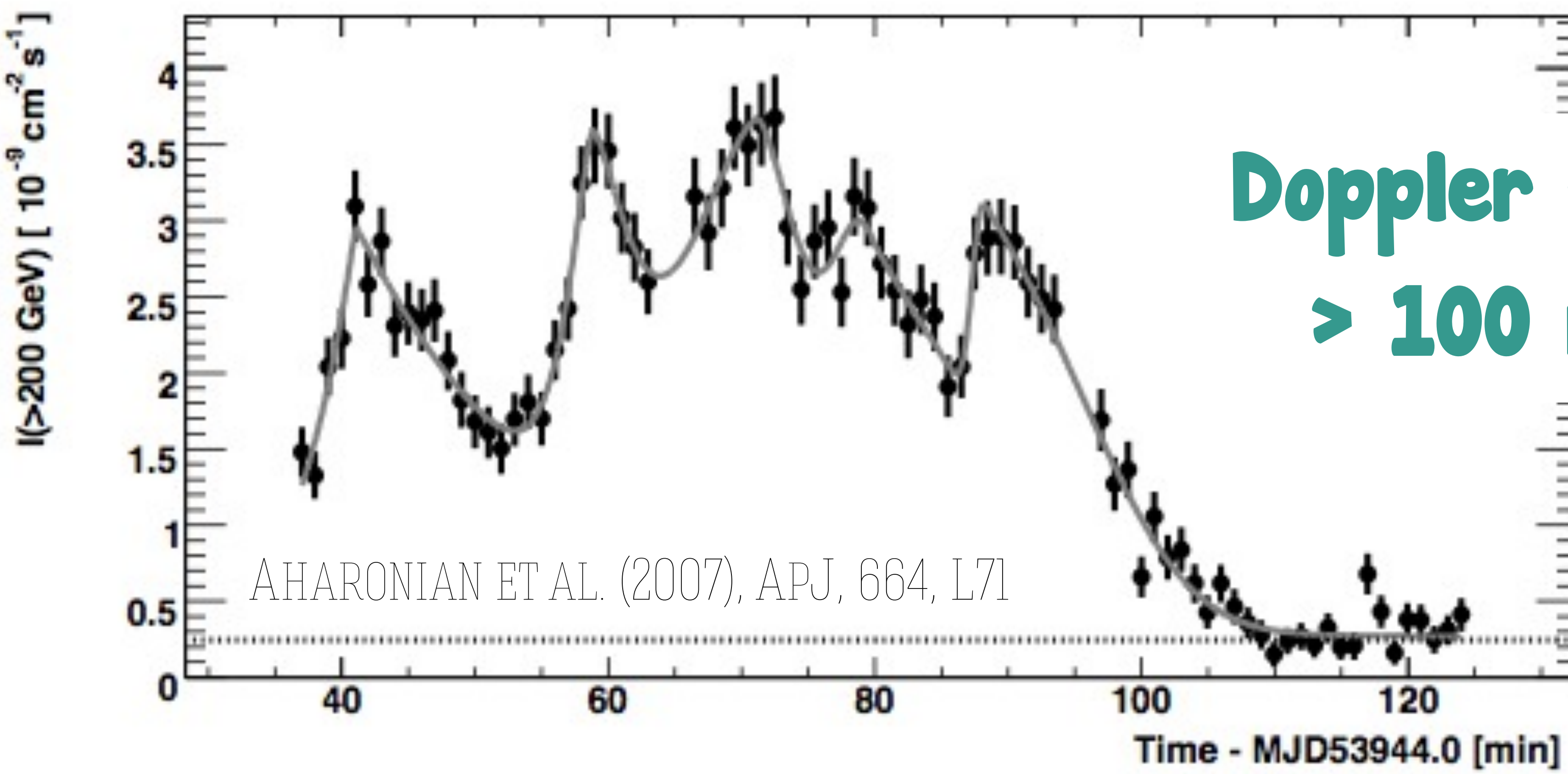

Doppler factors of > 100 required

Models of blazar emission

Krawczynski et al. (2004), ApJ 601, 151

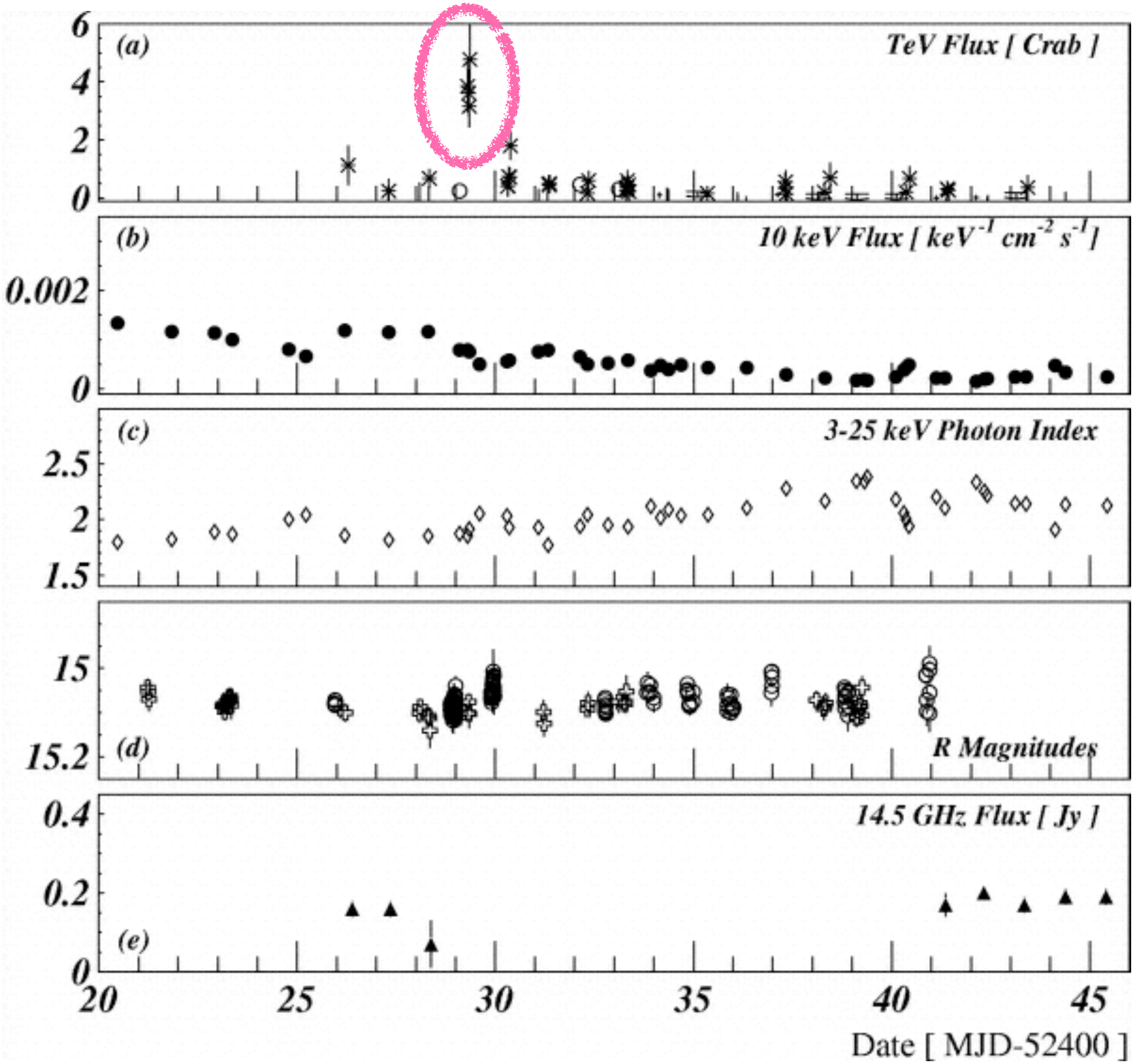

"orphan" flare from TeV blazar, 1ES 1959+650

hadronic models have been invoked to explain this behaviour

E.g., Boettcher (2005), ApJ, 621, 176
Sahu et al. (2013), Phys. Rev. D
... (in press) astro-ph/1305.4985

Models of blazar emission

H.E.S.S. COLLABORATION ET AL. (2013 - IN PRESS) DAVID SANCHEZ & PASCAL FORTIN

- VHE emission discovered by H.E.S.S. (ATel July 2010)
- Hard Fermi spectrum (2.1) and nearby (z=0.049)

➡ excellent candidate for TeV emission

- X-ray observations taken simultaneously with VHE reveal onset of HE component at unusually low energies for a TeV BL Lac

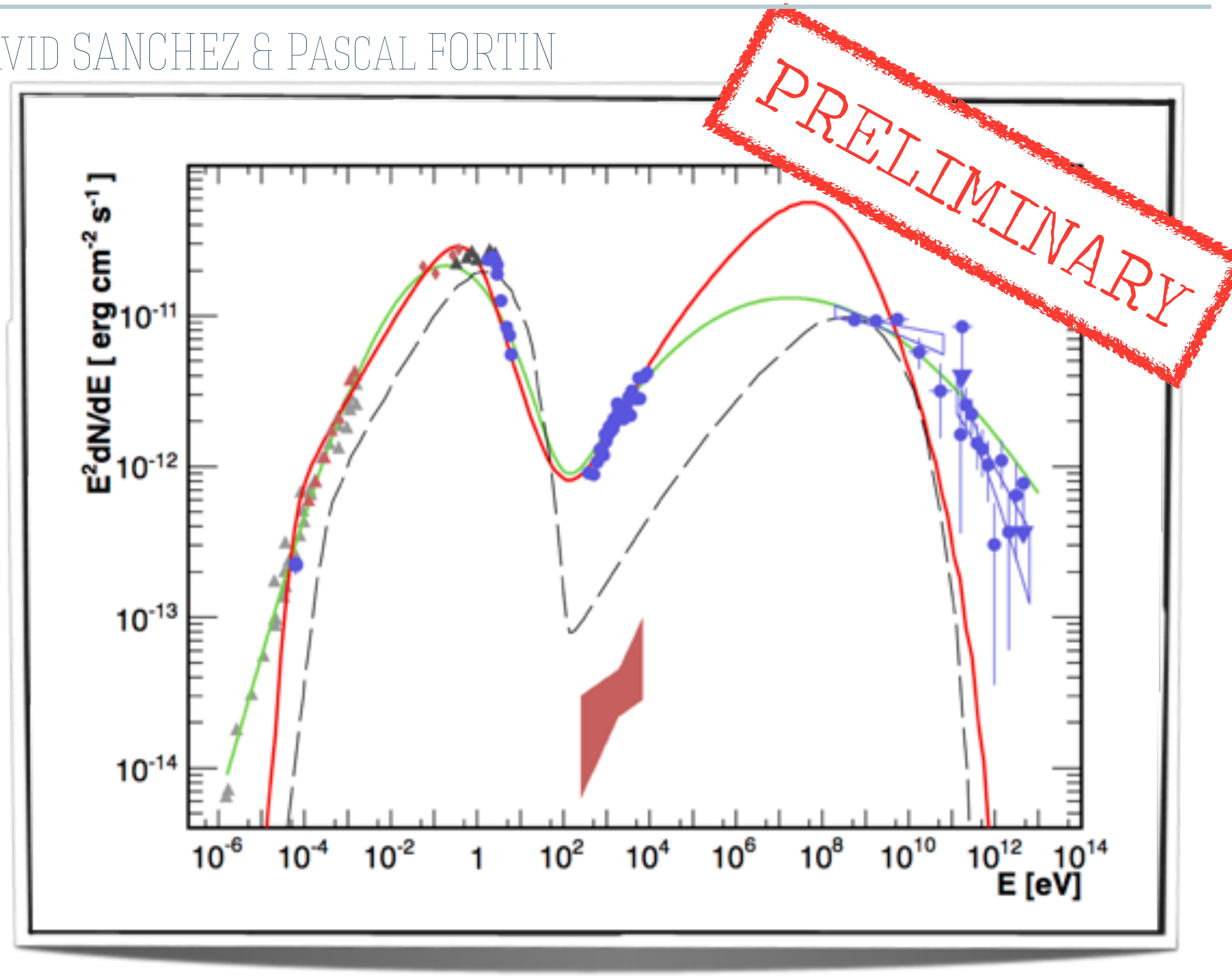

Models of blazar emission

H.E.S.S. Collaboration et al. (2013 - in press) David Sanchez & Pascal Fortin

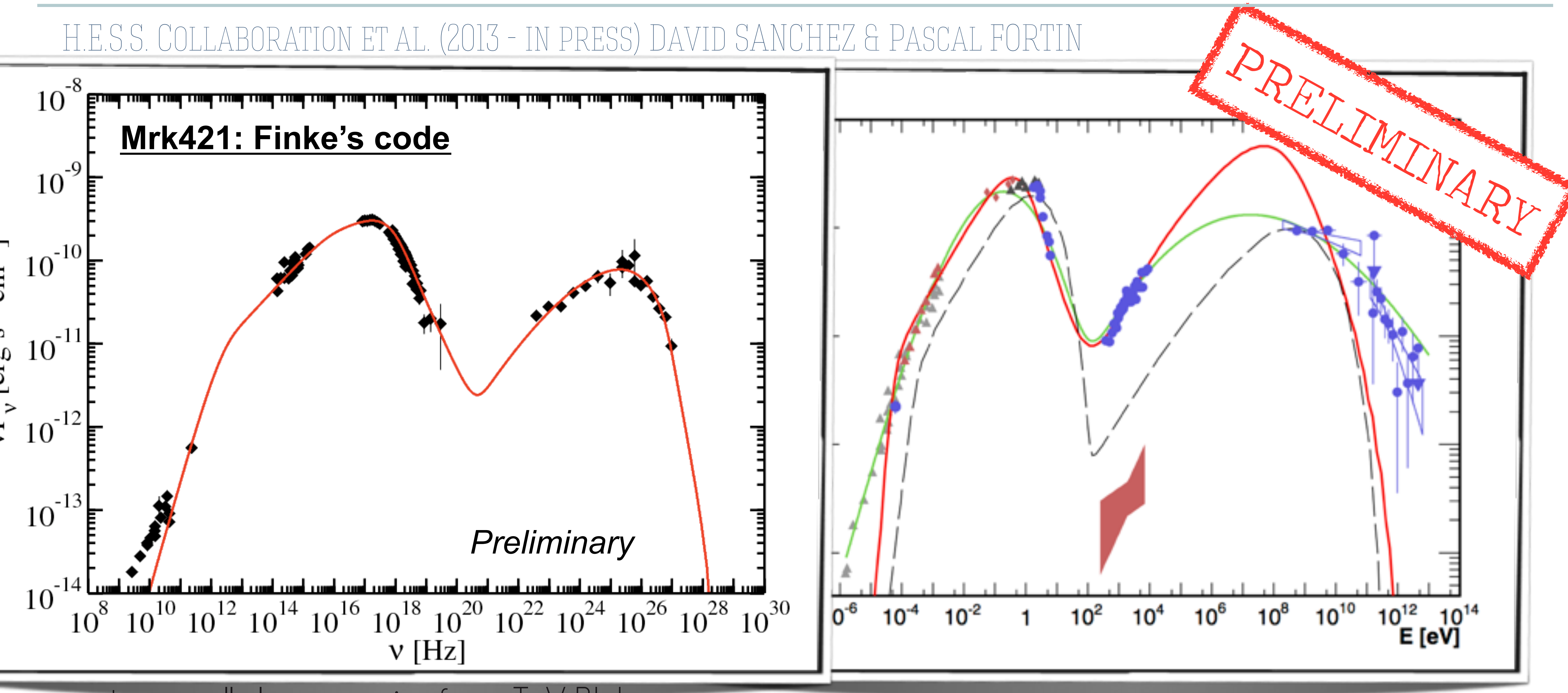

at unusually low energies for a TeV BL Lac

Models of blazar emission

H.E.S.S. Collaboration et al. (2013 - in press) David Sanchez & Pascal Fortin

- VHE emission discovered by H.E.S.S. (ATel July 2010)
- Hard Fermi spectrum (2.1) and nearby (z=0.049)

➡ excellent candidate for TeV emission

- X-ray observations taken simultaneously with VHE reveal onset of HE component at unusually low energies for a TeV BL Lac

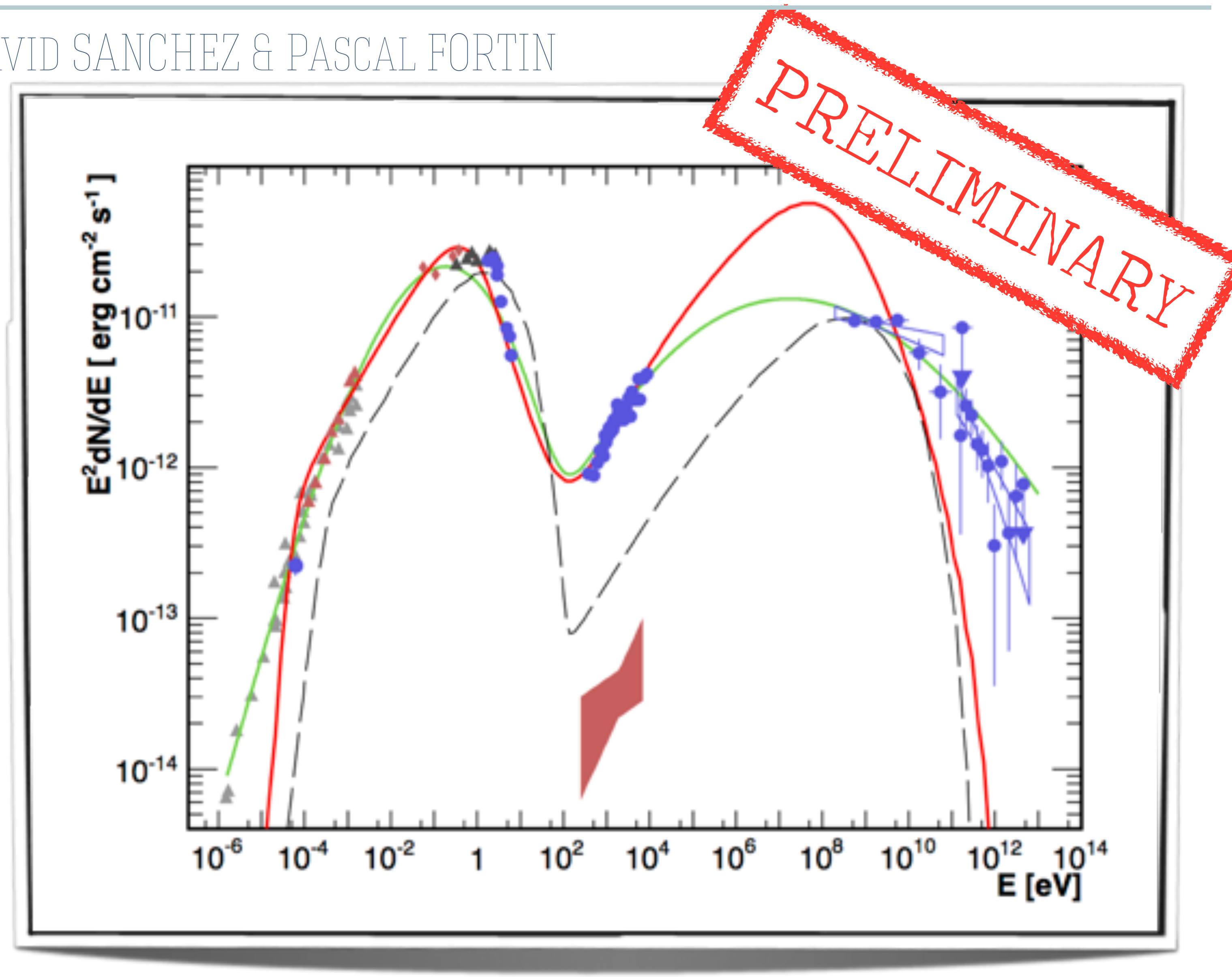

Difficult to model with a single zone homogeneous SSC model due to the unprecedented width of the HE component compared to the LE component

The Fermi blazars
4/9

The Fermi blazars

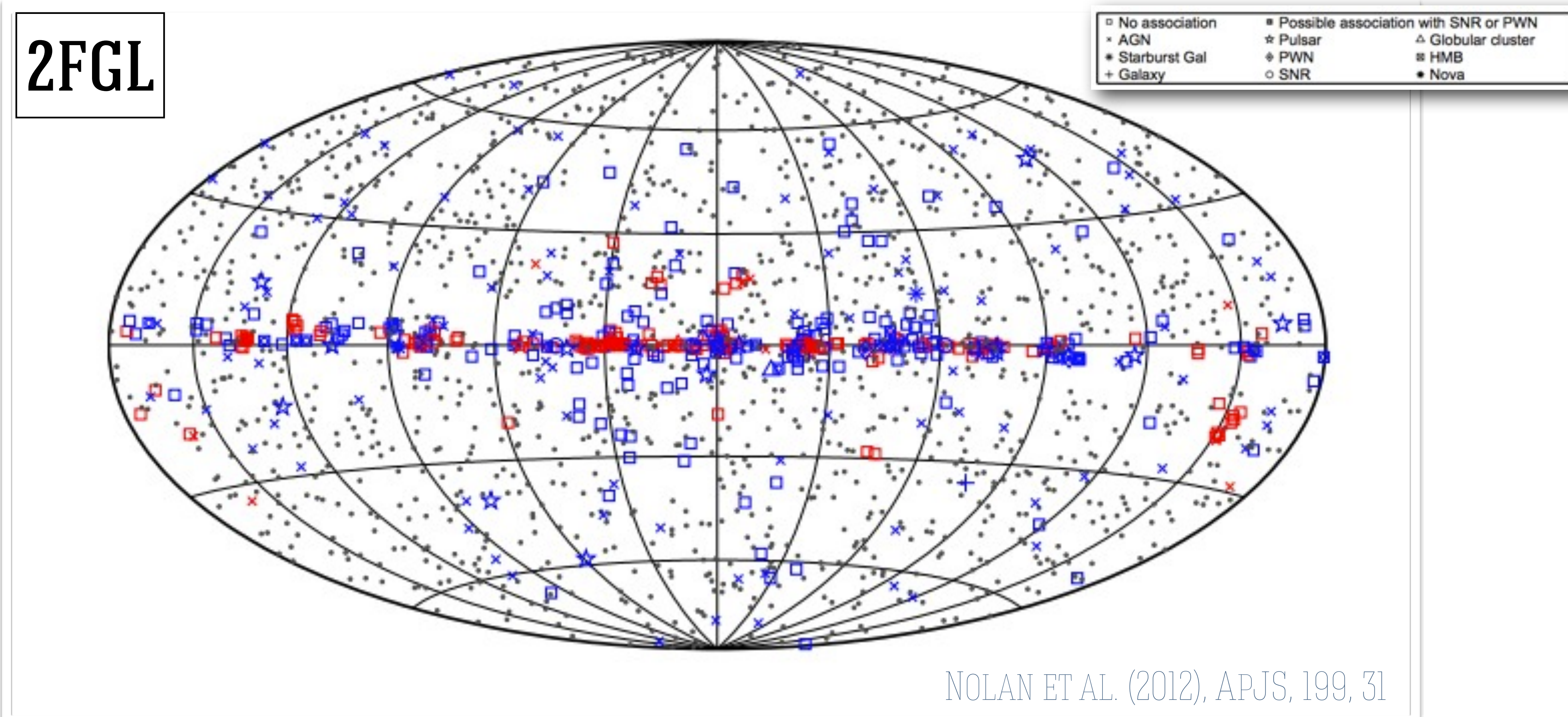

NOLAN ET AL. (2012), APJS, 199, 31

1873 SOURCES

1298 IDENTIFIED/ASSOCIATED

84%

AGN*

*74% blazars

The Fermi blazars

1 **LBAS** (Abdo et. al 2009, ApJ 700, 597)
Based on 0FGL, 3 months data, ~10σ
106 high-confidence blazars

2 **1LAC** (Abdo et. al 2010, ApJ 715, 429)
Based on 1FGL, 11 months data, ~5σ
523 (blazars) / 599 (total) in clean sample

3 **2LAC** (Ackermann et. al 2011, ApJ 743, 171)
Based on 2FGL, 24 months data, ~5σ
862 (blazars) / 886 (total) in clean sample

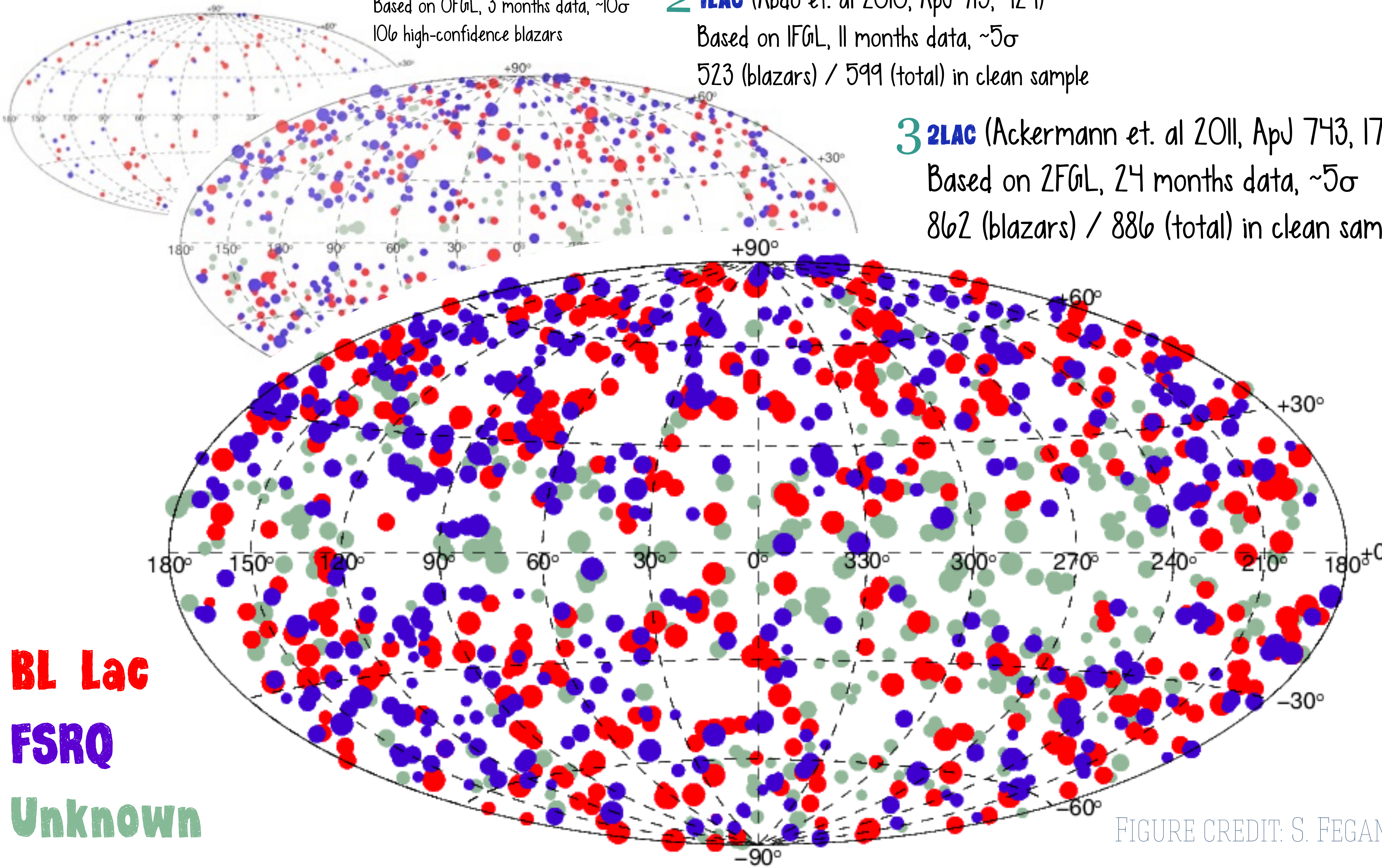

BL Lac
FSRQ
Unknown

Figure credit: S. Fegan

The Fermi blazars

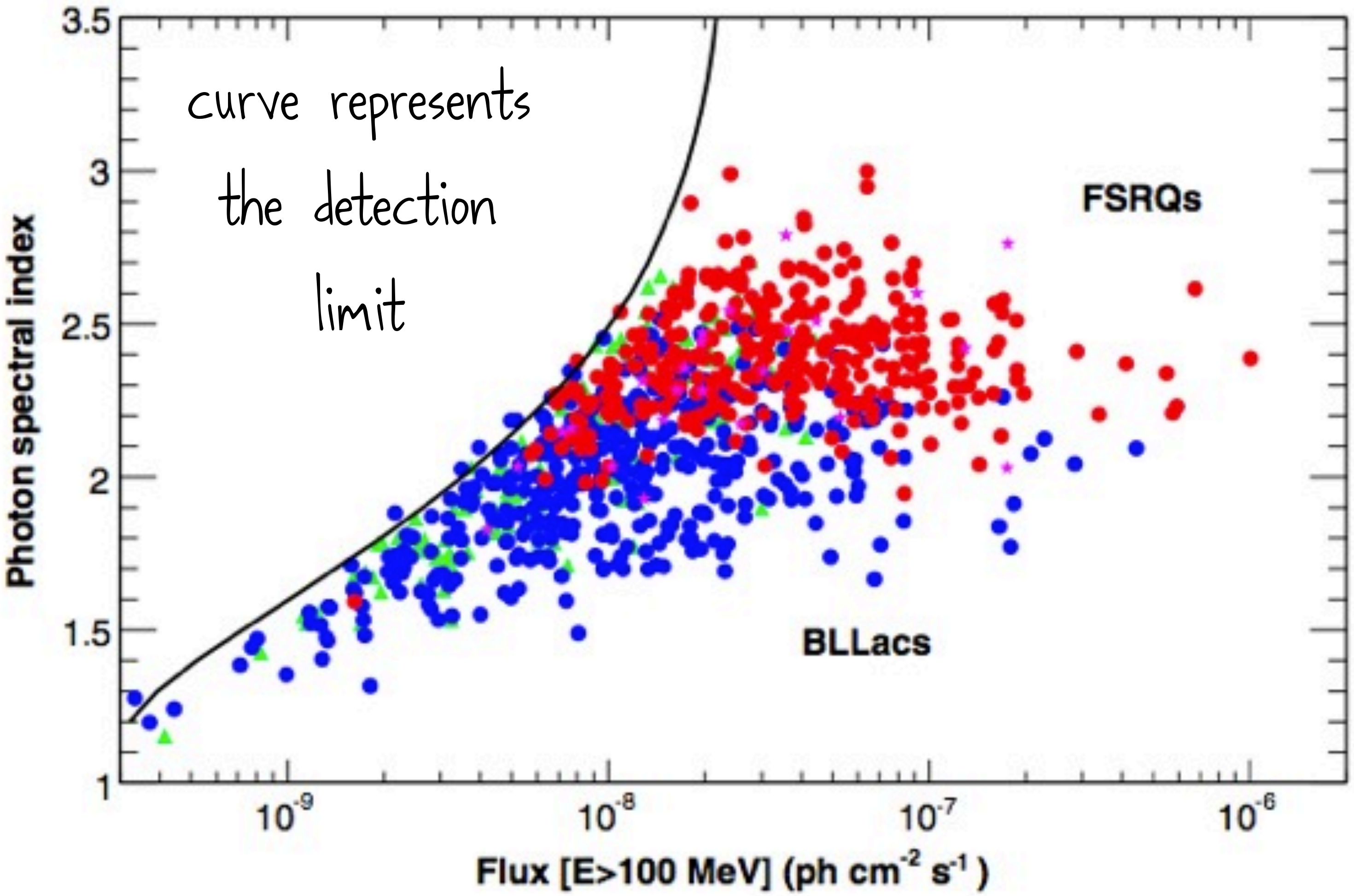

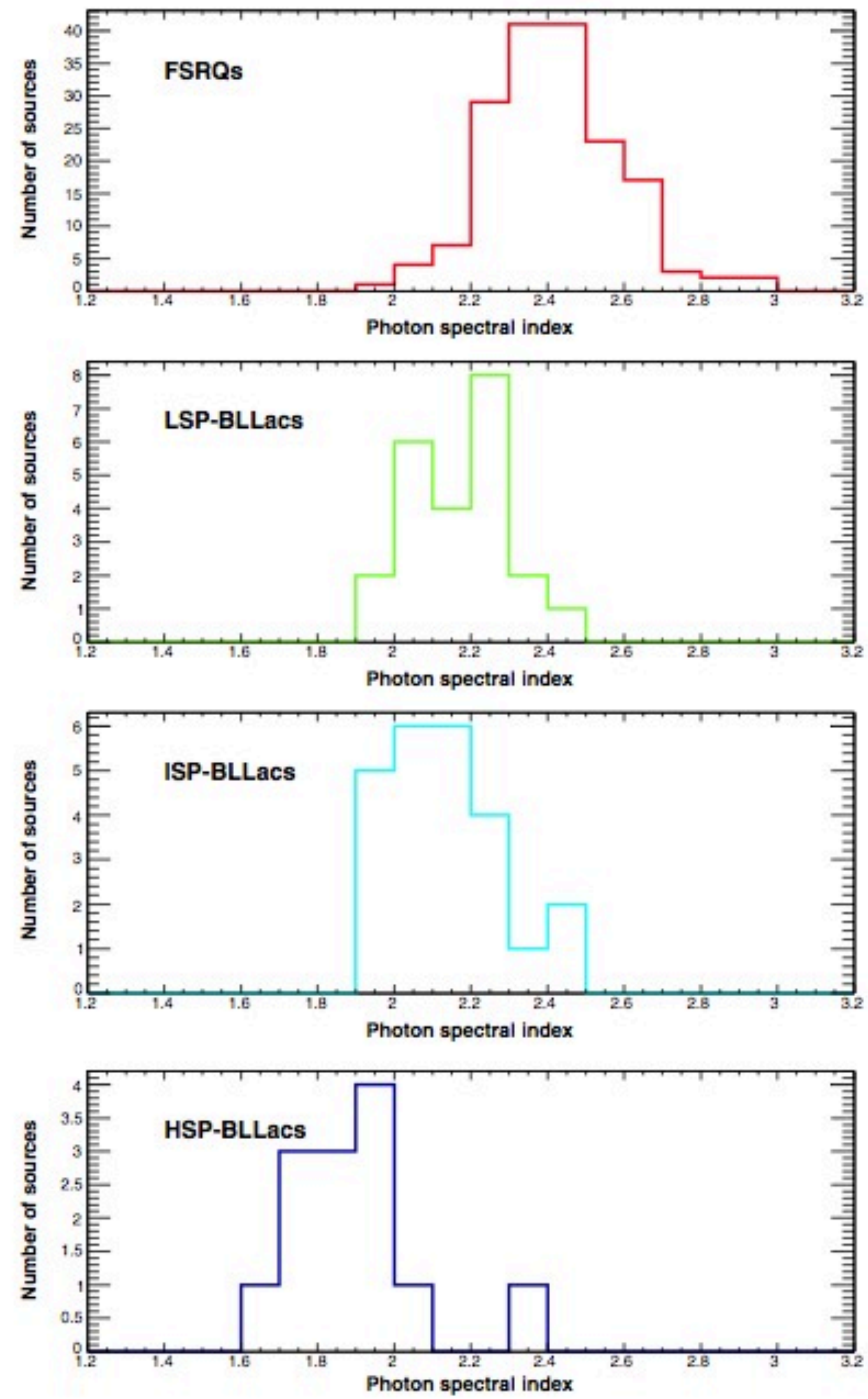

ACKERMANN ET. AL 2011, APJ 743, 171

The Fermi blazars

Table 5
Census of Sources

AGN Type	Entire 2LAC	2LAC Clean Sample[a]	Low-lat Sample
All	1017	886	104
FSRQ	360	310	19
LSP	246	221	7
ISP	4	3	2
HSP	2	0	0
No classification	108	86	10
BL Lac	423	395	16
LSP	65	61	3
ISP	82	81	3
HSP	174	160	5
No classification	102	93	5
Blazar of unknown type	204	157	67
LSP	24	19	10
ISP	13	11	3
HSP	65	53	13
No classification	102	74	41
Other AGNs	30	24	2

Note. [a] Sources with single counterparts and without * analysis flags. See Section 5 for the definitions of this sample.

ACKERMANN ET. AL 2011, APJ 743, 171

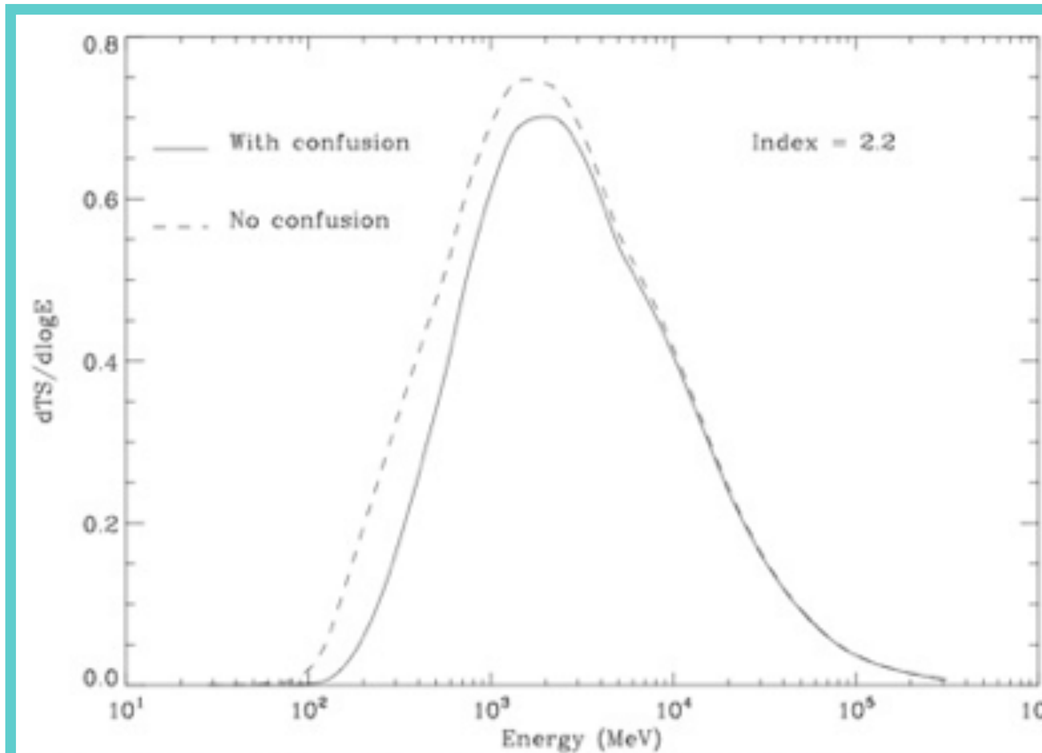

Figure 18. Theoretical contribution ($W(E)$ of Equation (A3)) to TS per Ms and per log(E) interval as a function of energy for a power-law source over the average background at $|b| > 10°$. The assumed photon spectral index is 2.2. The dashed line is for an isolated source. The full line includes approximately the effect of source confusion.

ABDO ET. AL 2010, APJS 188, 405

*8 misaligned blazars
4 NLSyls
10 AGN of other type
2 starbursts

The Fermi blazars

Fossati et al. (1998), MNRAS, 299, 433

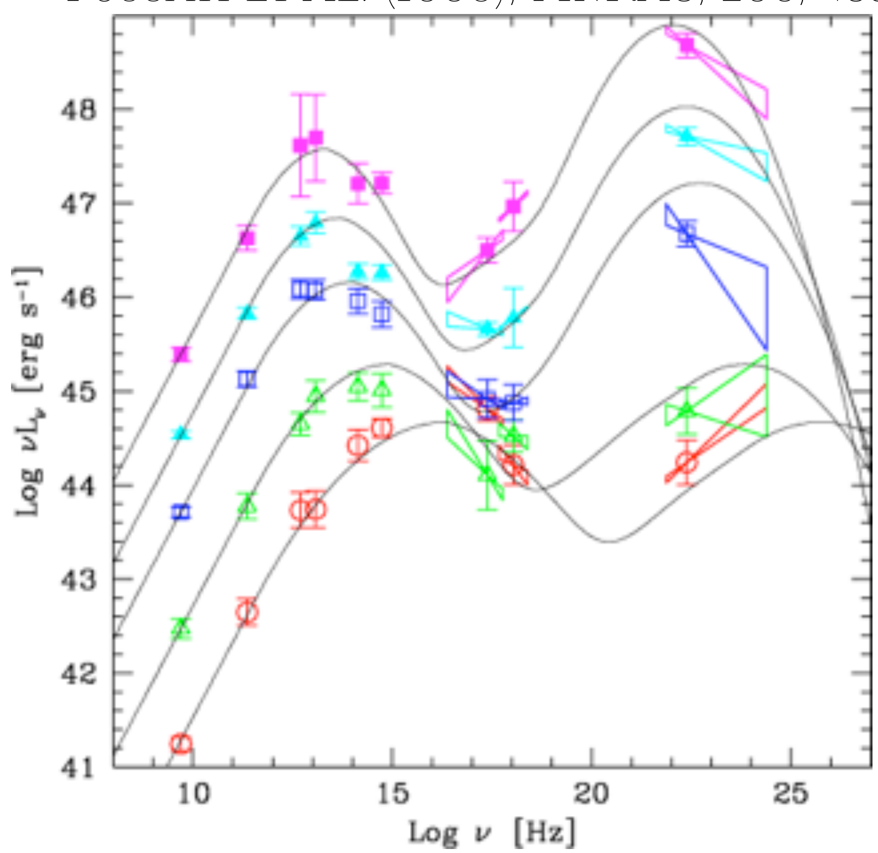

Finke, J. (2012), Fermi-Jansky (astro-ph/1301.6081)

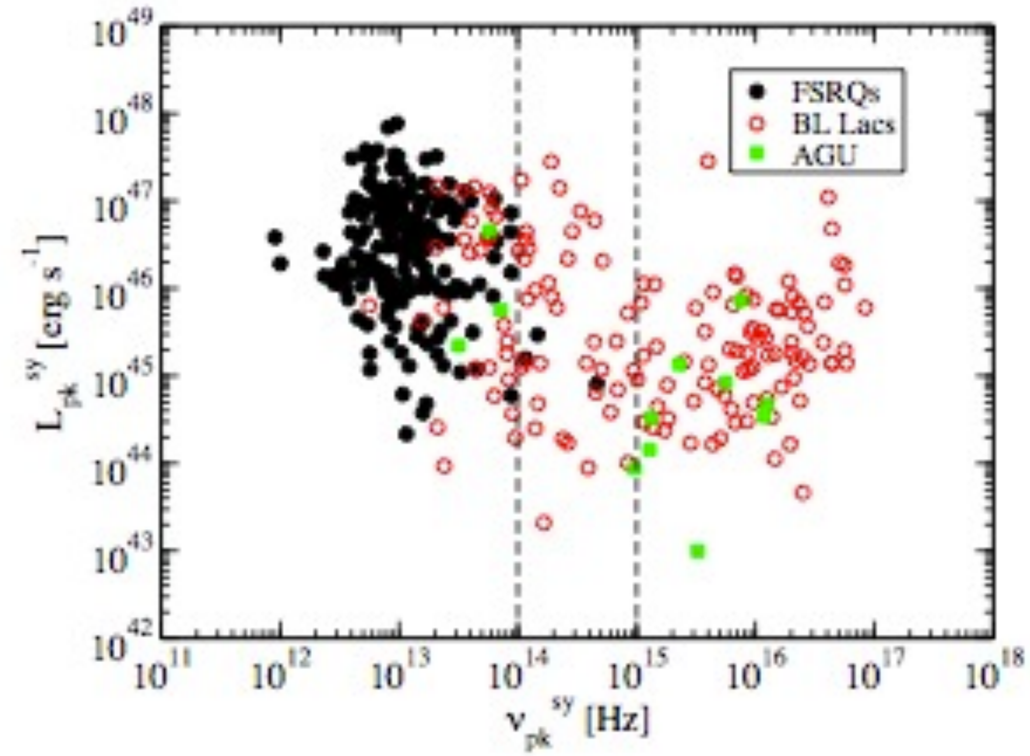

"If the seed photon source for external Compton scattering is the broad line region (BLR), and the BLR strength is correlated with the power injected into electrons in the jet, one would expect that more luminous jets have stronger broad emission lines and greater Compton cooling, and thus a lower ν_{sy}. As the power injected in electrons is reduced, the broad line luminosity decreases, there are fewer seed photons for Compton scattering, and consequently the peak synchrotron frequency moves to higher frequencies. This is also reflected in the lower luminosity of the Compton-scattered component relative to the synchrotron component as ν_{sy} moves to higher frequencies." Finke, J. (2012), Fermi-Jansky (astro-ph/1301.6081)

The Fermi blazars

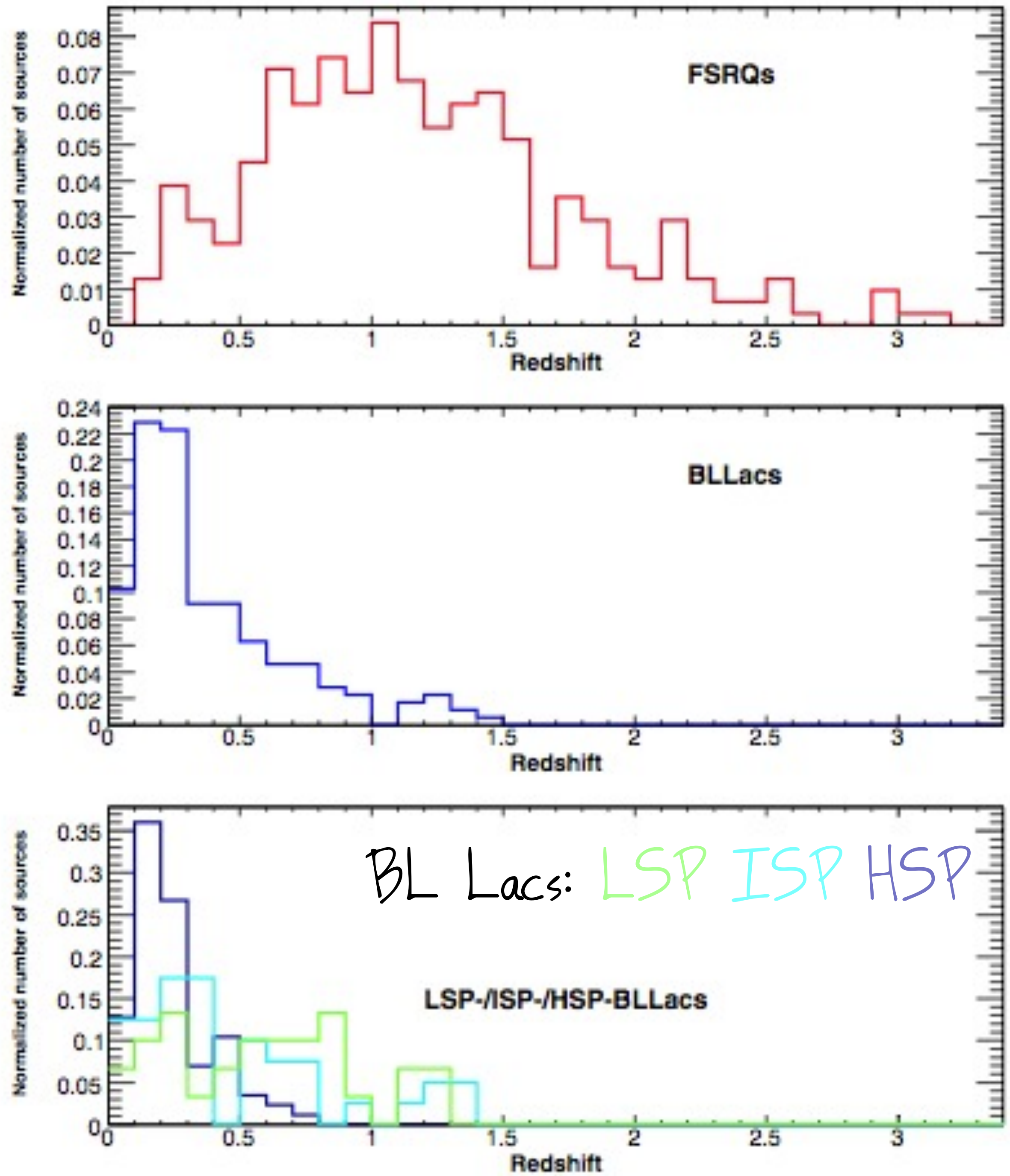

Ackermann et. al 2011, ApJ 743, 171

The Fermi blazars

The Hard Source List - a catalog above 10 GeV

D. Paneque, Fermi Symposium (2012)

- Work is underway to publish the 1st Fermi-LAT catalog of sources > 10 GeV
- Shape of the spectrum at > 10 GeV might not be well characterized if we use a single fit in the energy range 0.1 GeV - 100 GeV
  - ➡ Lower energies

See Lamb & Macomb (1997), 488, L872

- The variability at ... from that at the lowest energies, whic... tion of particles which may radiate from the same/different location
  - ➡ Are sources more variable at HE than at LE ? or the other way around ?
- **Understand better the population of sources emitting above 10 GeV**
  - ➡ What are the sources dominating the highest LAT energies?
- **IDENTIFY PROMISING CANDIDATES FOR IACTS ... NEW VHE DISCOVERIES**

The TeV blazars
5/9

The TeV blazars

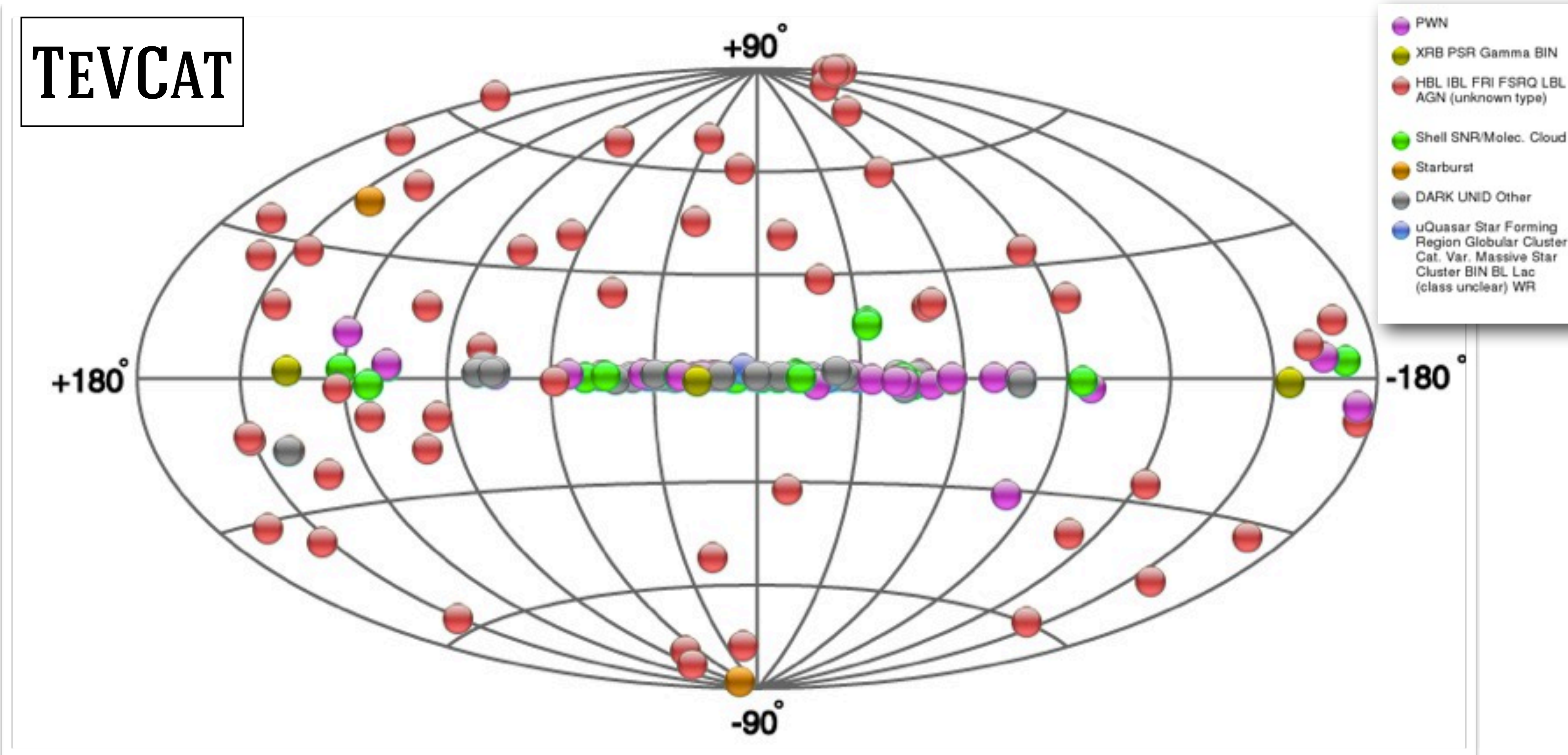

145 sources
114 identified/associated

84%
AGN*

*95% blazars

The TeV blazars

As of writing this talk, there are 145 sources in TeVCat – 57 Extragalactic

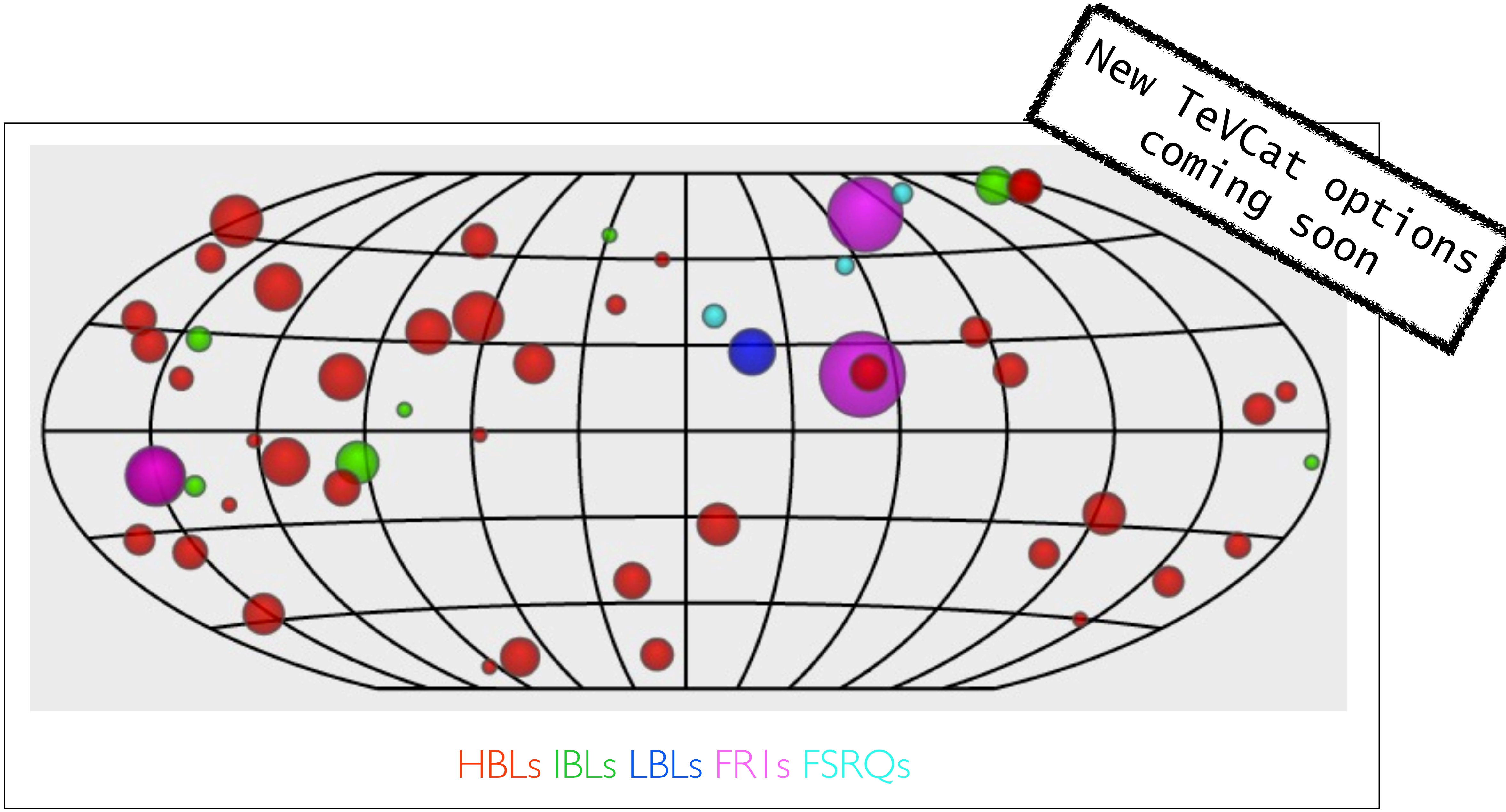

The TeV blazars

As of writing this talk, there are 145 sources in TeVCat - 57 Extragalactic

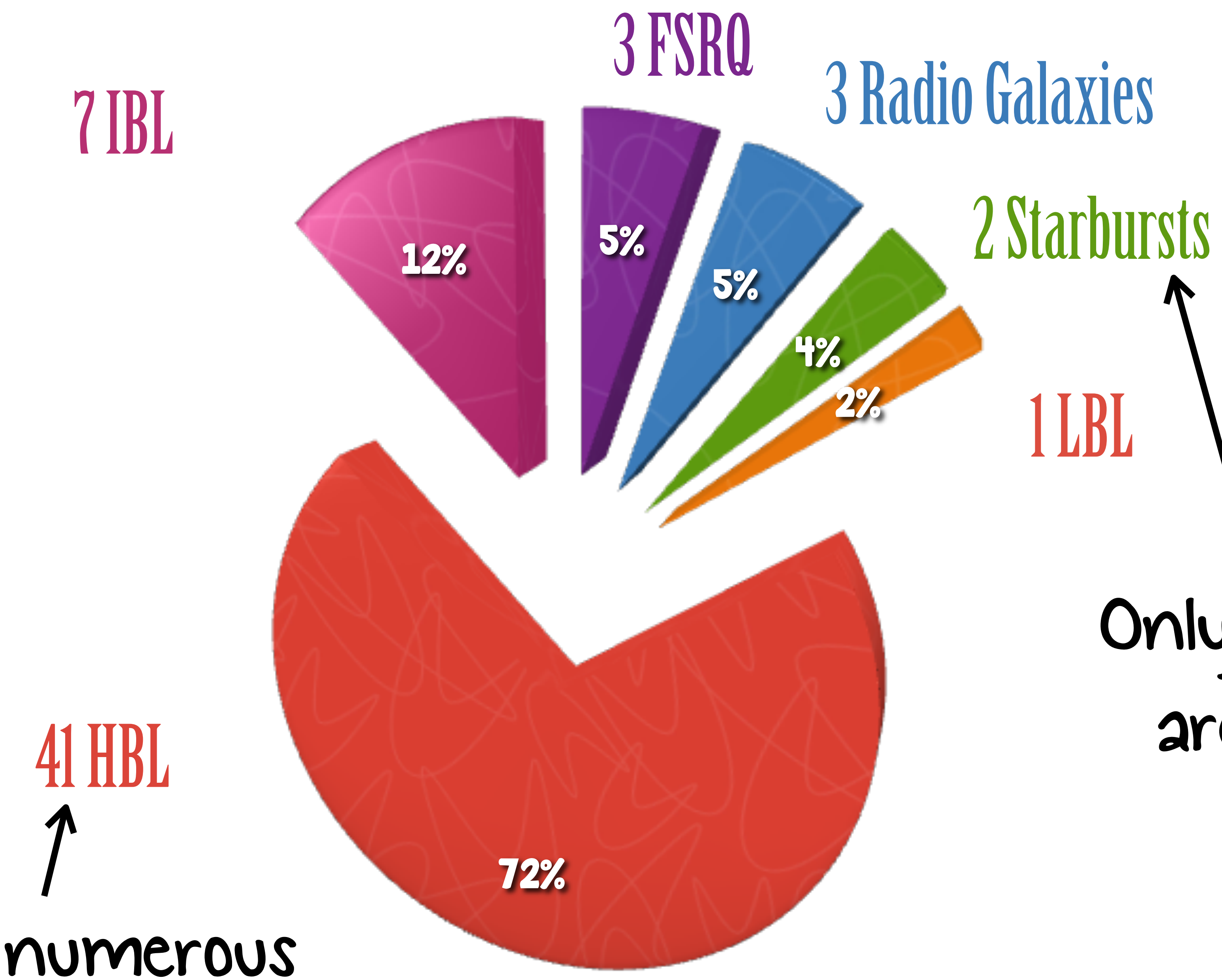

Only two sources are not AGN!

Most numerous source class in TeV sky

The GeV-TeV Connection
6/9

The GeV-TeV Connection

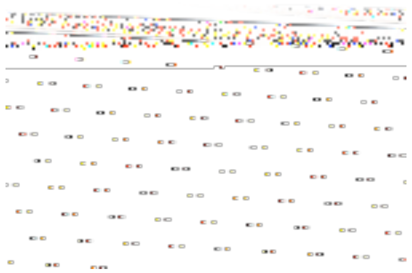

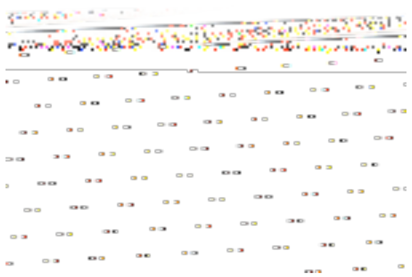

	Total No. Sources	Total No. Identified*	No. AGN	% AGN that are blazars
GeV ... Fermi 2FGL	1873	1298 (69%)	1092 (84%)	74%
TeV ...TeVCat	145	117 (81%)	55 (47%)	96%

*Identified / Associated

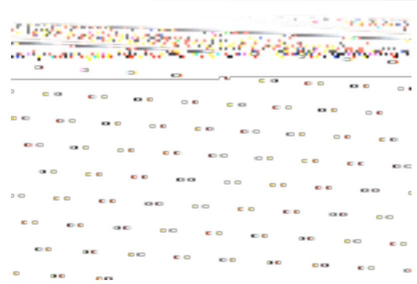

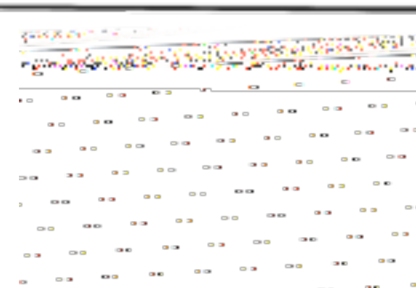

49 of the 55 TeV AGN are in 2FGL

The GeV-TeV Connection

Senturk, Errando, Böttcher & Mukherjee (2013), ApJ 764, 119

- **Analysed 27 months of Fermi data for the TeV AGN that had spectral infrormation available (26 objects)**
- Compared the TeV AGN with the AGN from 2FGL
- Computed SEDs for all objects
- The combined GeV-TeV spectra of some blazars (1ES 0229+200, 1ES 0347-121, 1ES 1101-232, 1ES 1218+304, H 1426+428) suggest an inverse-Compton peak beyond 1 TeV

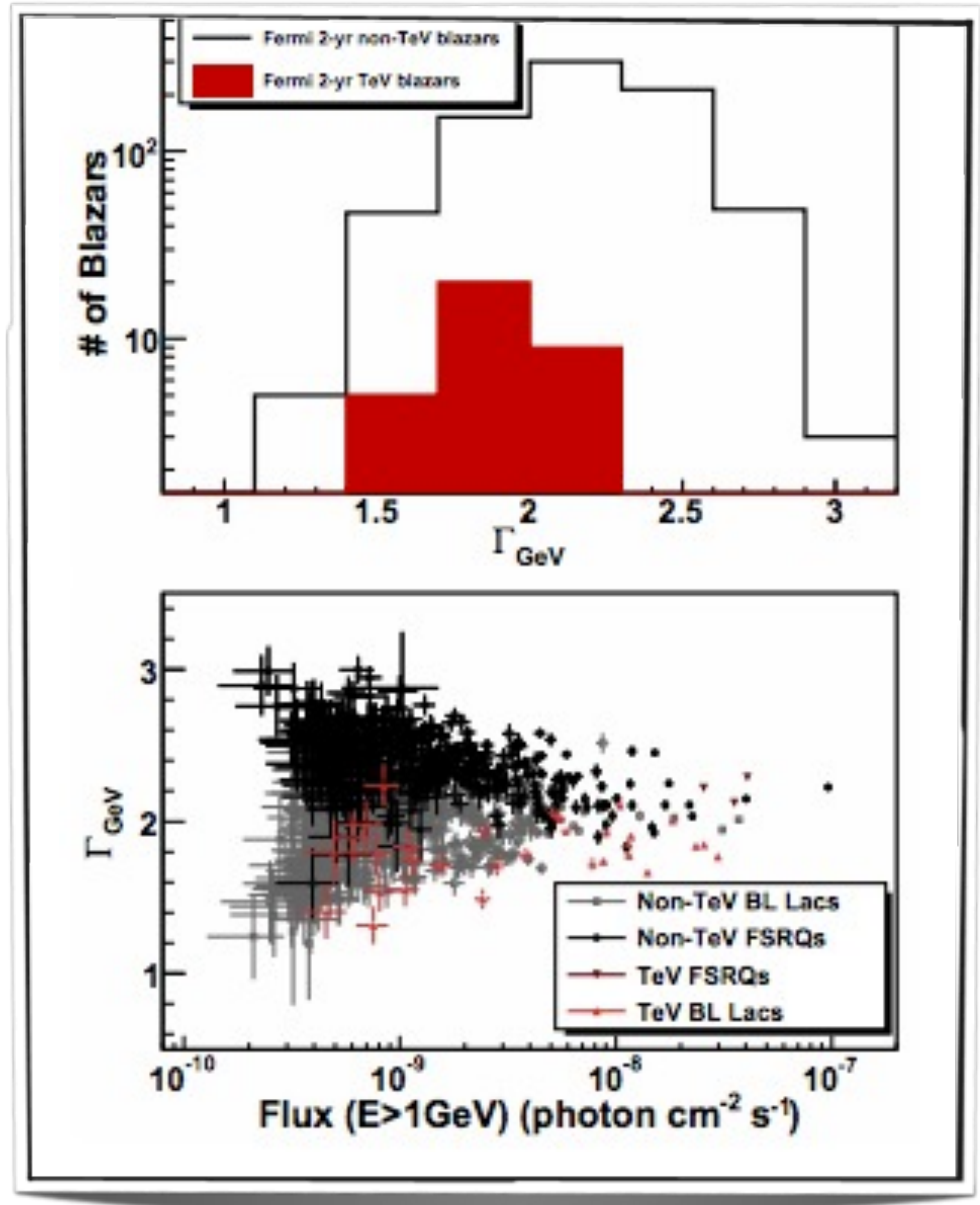

The GeV-TeV Connection

- TeV instruments are pointed and have relatively small fields of view
- Low duty cycles (~10%)

➡ **Need targets**

- Fermi has a very large field of view - sees a fifth of the sky at any given time
- Surveys entire sky every three hours

➡ **Transients, cataloging**

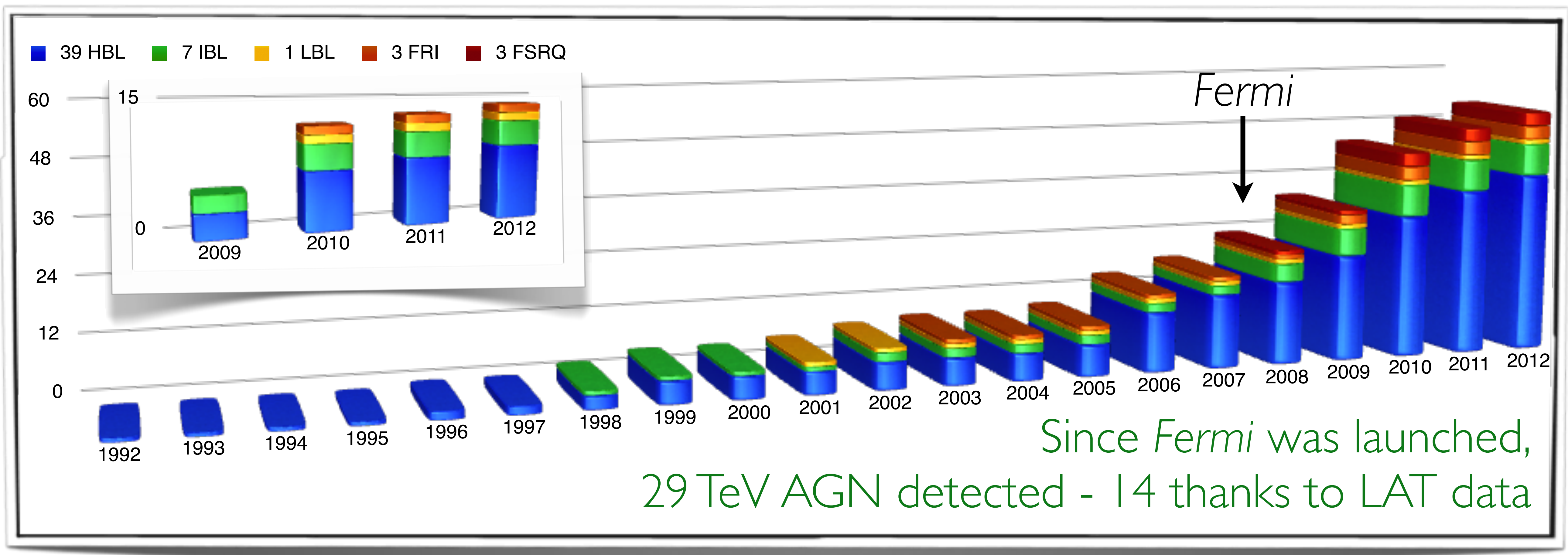

The GeV-TeV Connection

- At the time of publication, there were 6 TeV AGN that were not detected in 2FGL
- Since then, 8 TeV AGN have been detected - they were all in 2FGL

  ➡ **still 6 TeV AGN not in 2FGL**

- all HBL
- among the weakest TeV AGN
- 3 have subsequently been reported as detections (non-Fermi pubs)


49 of the 55 TeV AGN are in 2FGL

Name	Class	% Crab
SHBL J001355.9-185406	HBL	1.0
1ES 0229+200*	HBL	1.8
1ES 0347-121*	HBL	2.0
PKS 0548-322*	HBL	1.3
1ES 1312-423	HBL	0.4
HESS J1943+213	HBL	1.5

*Detections reported in the literature since 2FGL

The extragalactic background light
7/9

The extra-galactic background light

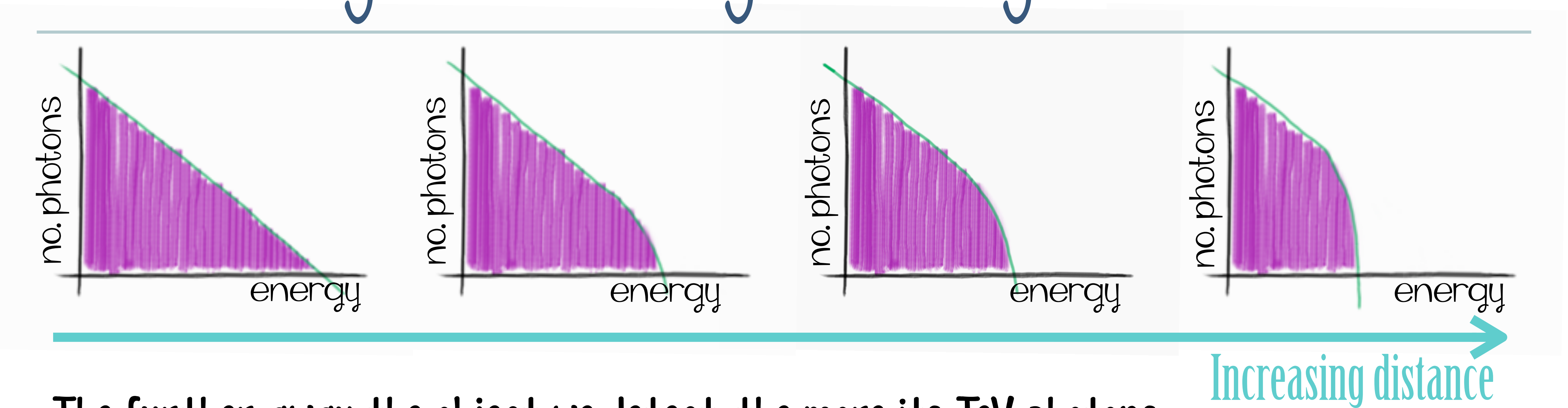

The further away the object we detect, the more its TeV photons are absorbed by the EBL - this results in a break in the spectrum

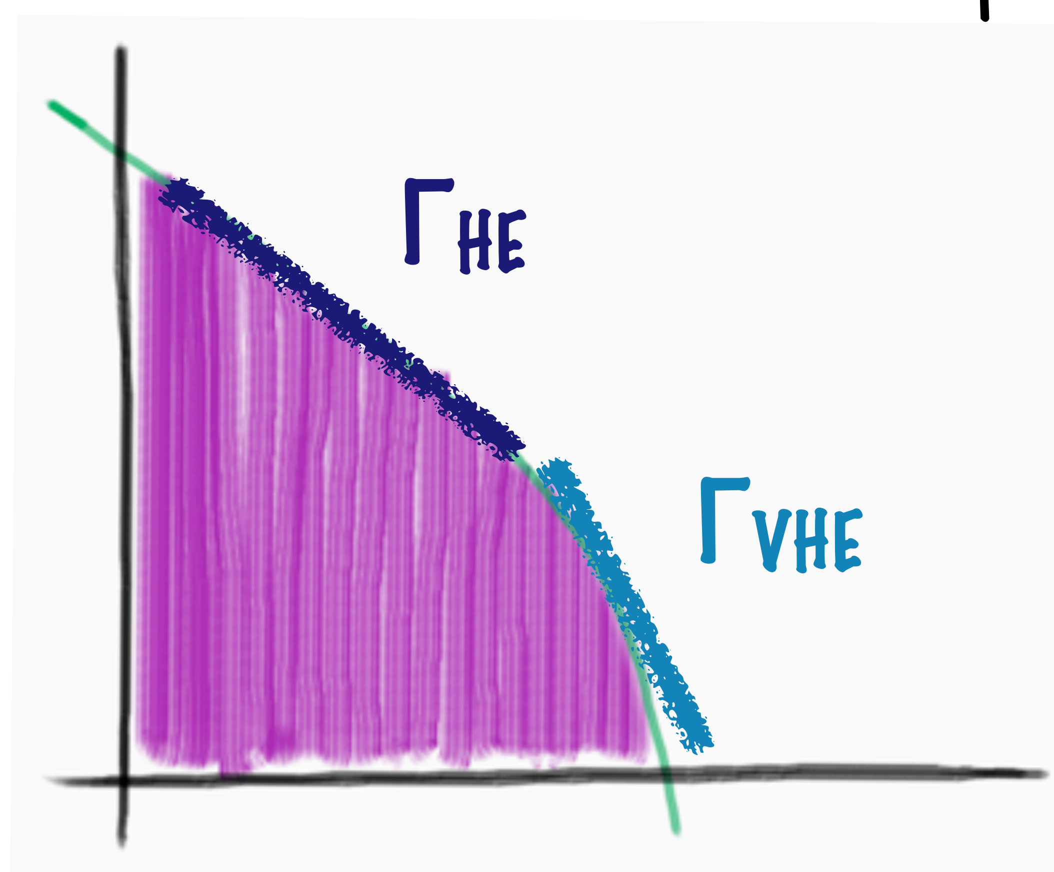

The extra-galactic background light

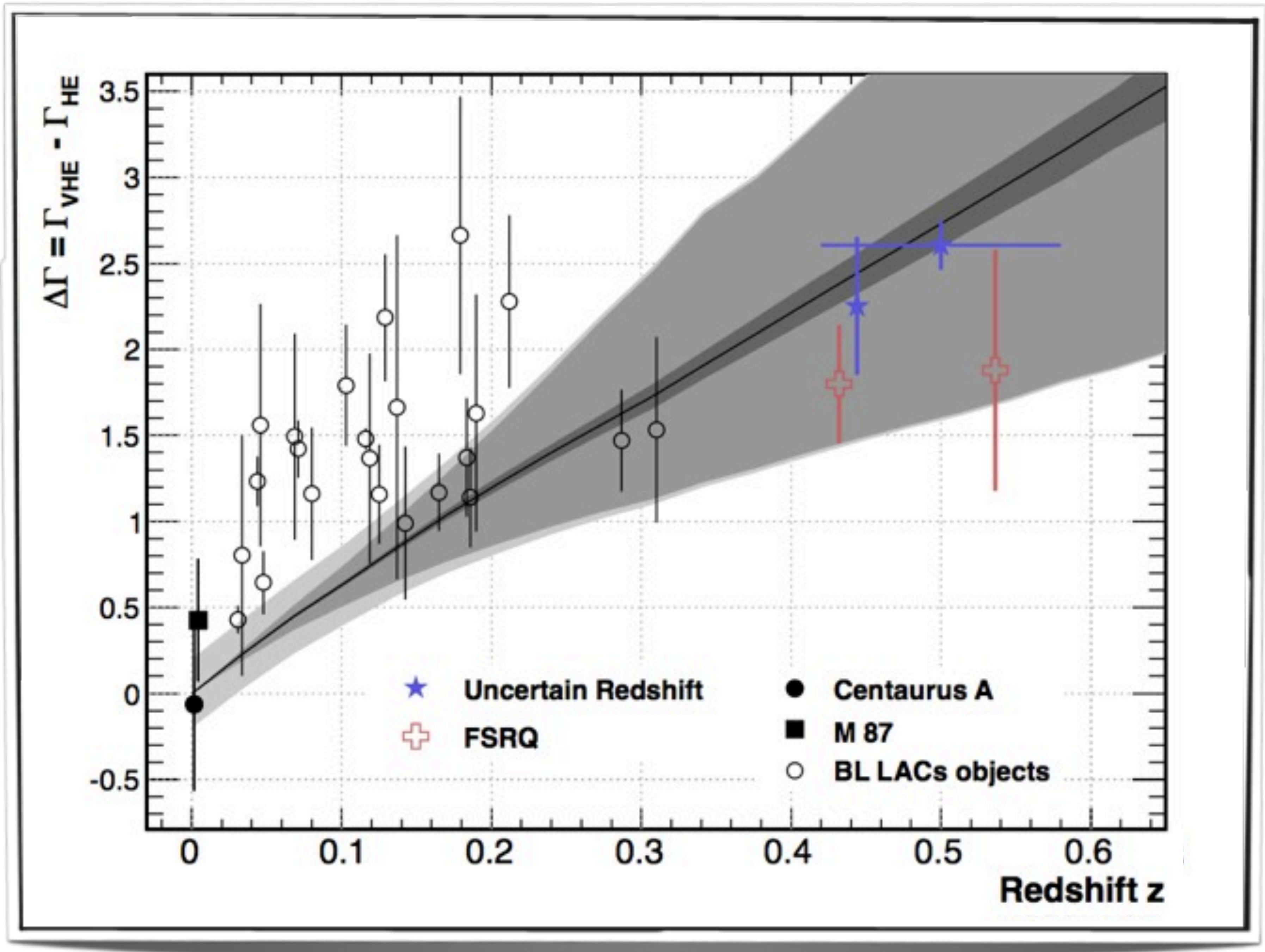

Abdo et al. (2009), ApJ, 707, 1310

Sanchez, Fegan, Giebels (2013) in press, astro-ph/1303.5923

The extra-galactic background light

WWW.MPI-HD.MPG.DE ASTRO-PH/1212.3409

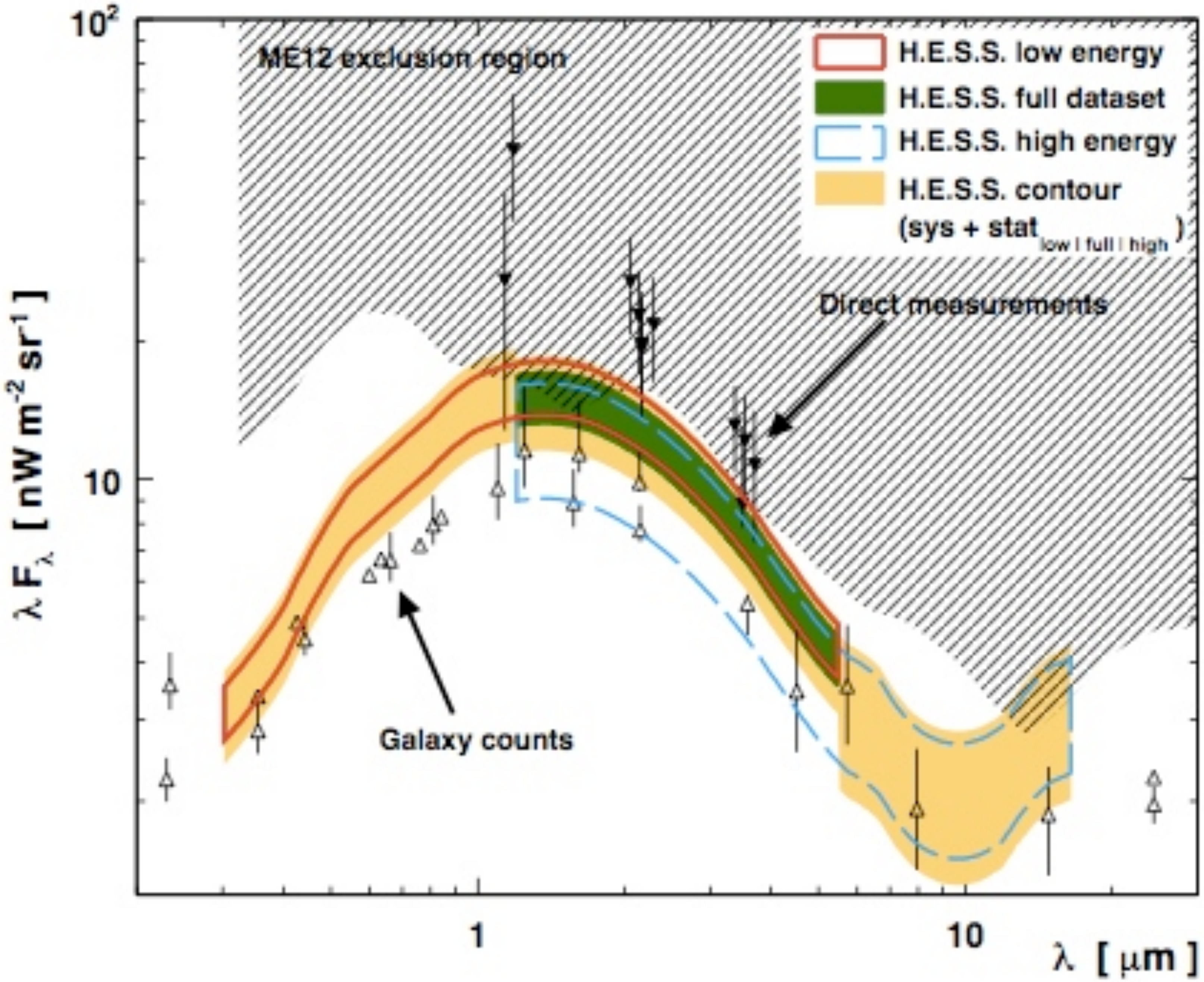

HESS data on seven blazars were used to search for the absorption signature of the EBL - it was detected at 9 sigma - results are only slightly above the lower limits calculated by summing galaxies visible in sky surveys

Intergalactic magnetic fields
8/9

Intergalactic magnetic fields

- when we detect TeV gamma rays from a distant source, we know that the signal has already been attenuated - only a fraction of those emitted arrive on Earth

- the gamma rays collide with photons of the EBL en route from the source and pair produce

➡ **if there were NO magnetic fields in the universe, these charged pairs would not get deflected, they would travel in original direction until they Compton upscattered an EBL photon to MeV-GeV energies***

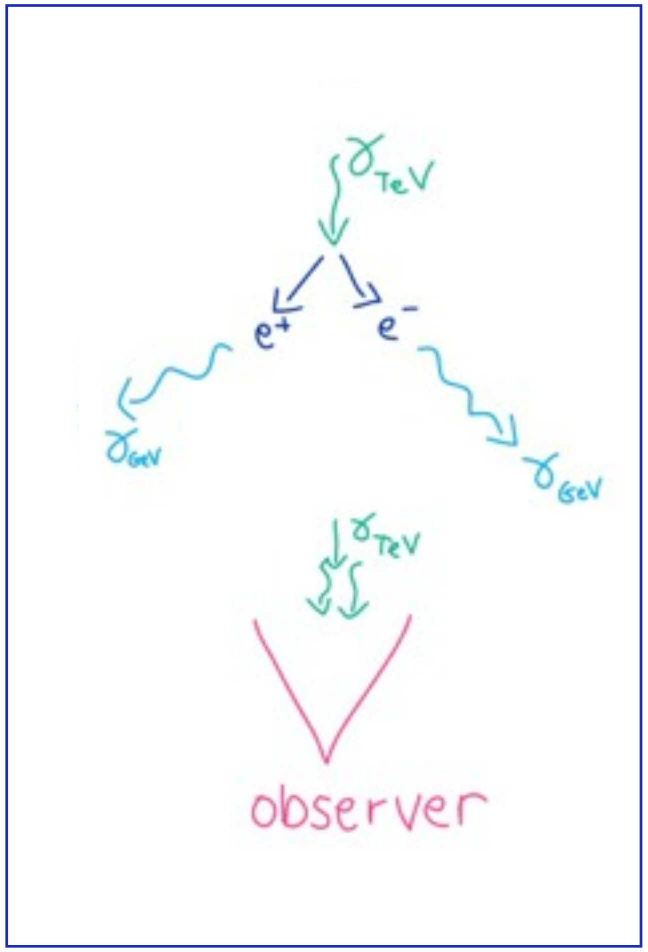

- in this way, the original TeV gamma rays get reprocessed to lower energy radiation

- IF we could identify a distant, steady** TeV source which had NO GeV emission, this could be an indication that the B-fields between the source and us deflected the charged pairs such that the reprocessed lower energy emission was "removed" (scattered) from the signal

* **the mean free path for e+/e- is low ~kpc** ** if the source is at a lower level now than when the TeV emission that we are detecting was emitted, it could be argued that, since the radiation due to the deflected pairs has longer to travel, it would be delayed by some time - and it hasn't arrived yet

Intergalactic magnetic fields

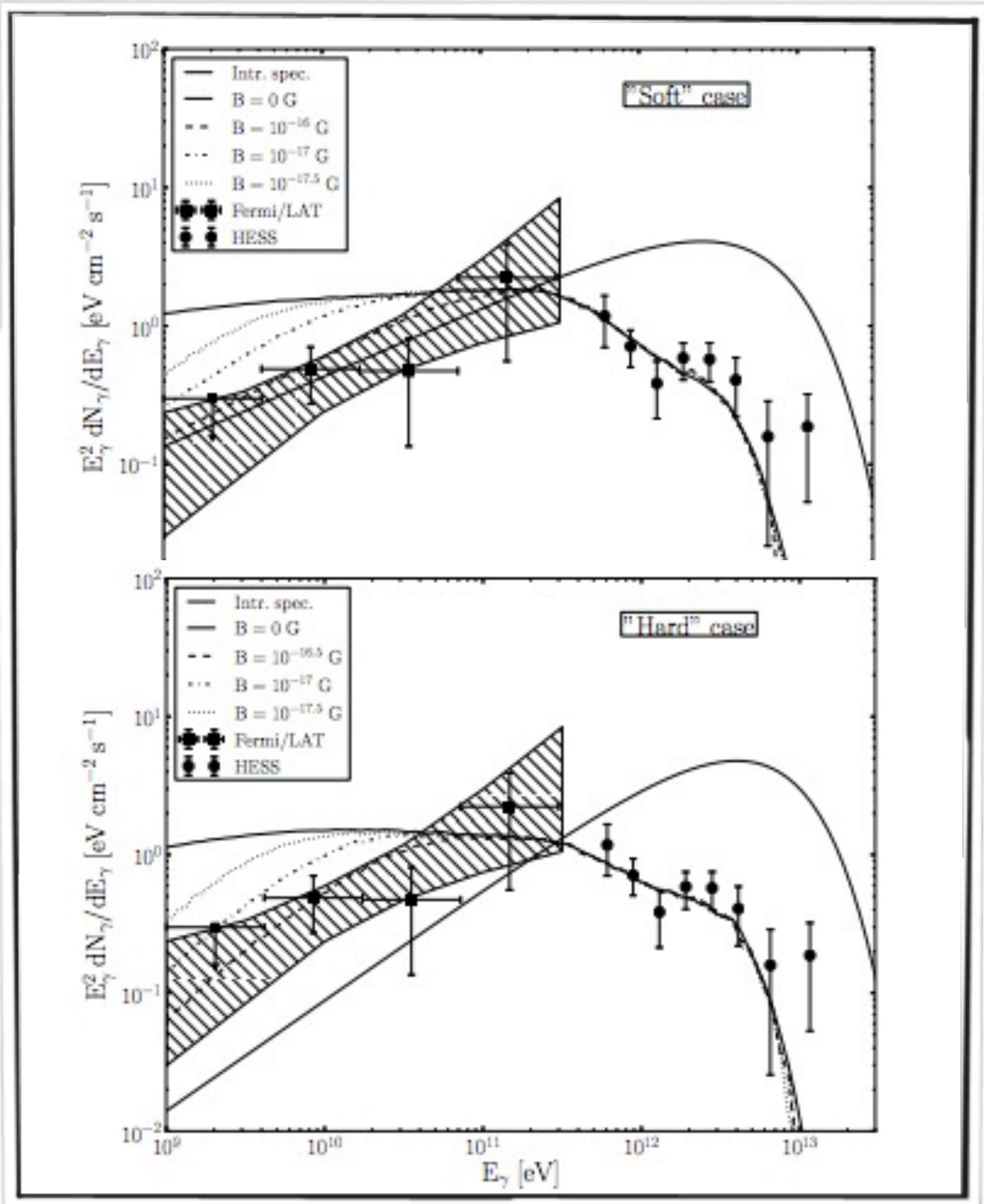

Vovk, Taylor, Semikoz & Neronov (2012), ApJ, 747, L14

Place constraints on the intergalactic B-field strength using the direct and cascade components of the GeV-TeV spectrum of 1ES 0229+200

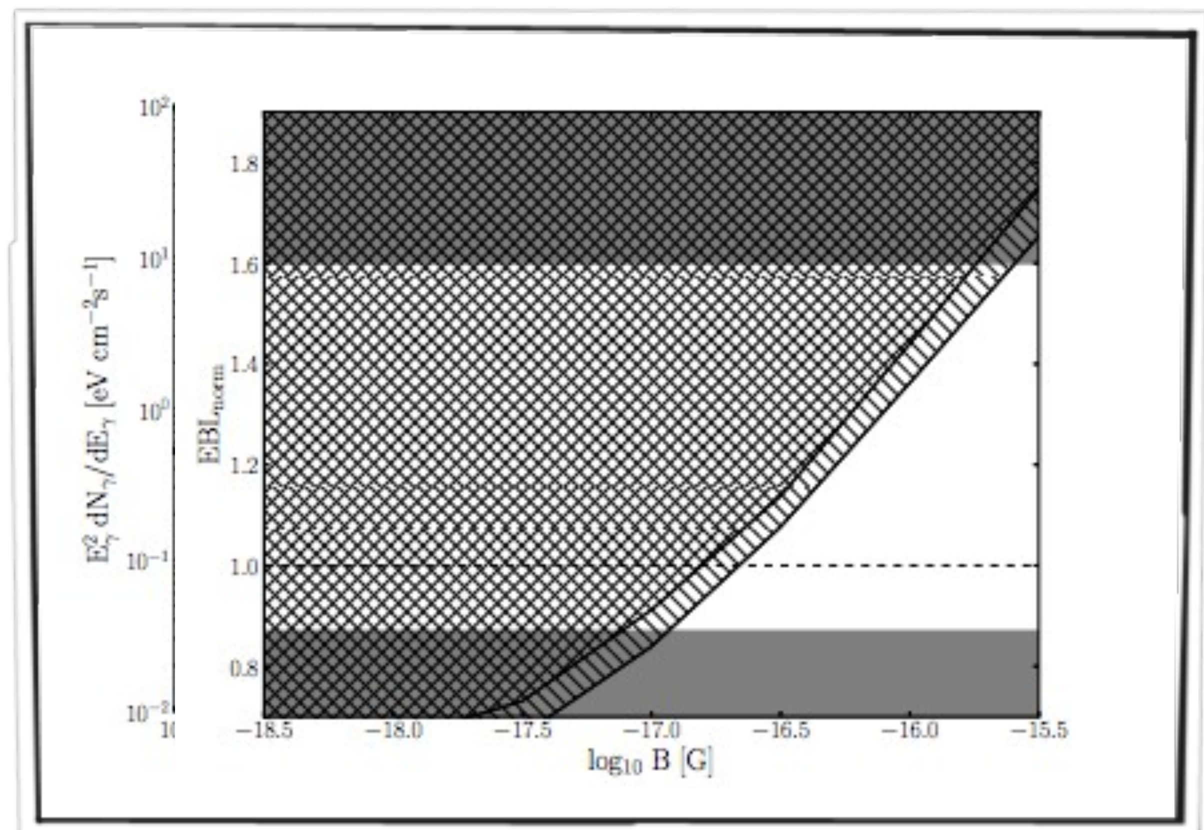

Characterising variability
9/9

Quantifying the variability of blazars

excess variance

Nandra et al. (1997) ApJ 476, 70

$$\sigma_{rms}^2 = \frac{1}{N\mu^2}\sum_{i=1}^{N}\left[(X_i-\mu)^2-\sigma_i^2\right]$$

N points in each light curve X_i

μ is the unweighted arithmetic mean of the X_i

Characterising variability

Putting an upper limit on the excess variance

➡ When no (negative) excess variance is measured in the data, we can estimate the level of intrinsic variance that could be present in the lightcurve but that would still allow us to arrive at this value for excess variance

1. Simulate lightcurves by generating, for each datapoint F_i +/− dF_i (F is the ith data point and dF is the ith uncertainty, i =1:N), a normal distribution centred on the mean of the measured lightcurve with width of sqrt(dF_i^2 + VARIANCE^2)

2. For each level of VARIANCE, generate a large number of lightcurves

Characterising variability

Sample lightcurves for different levels of VARIANCE

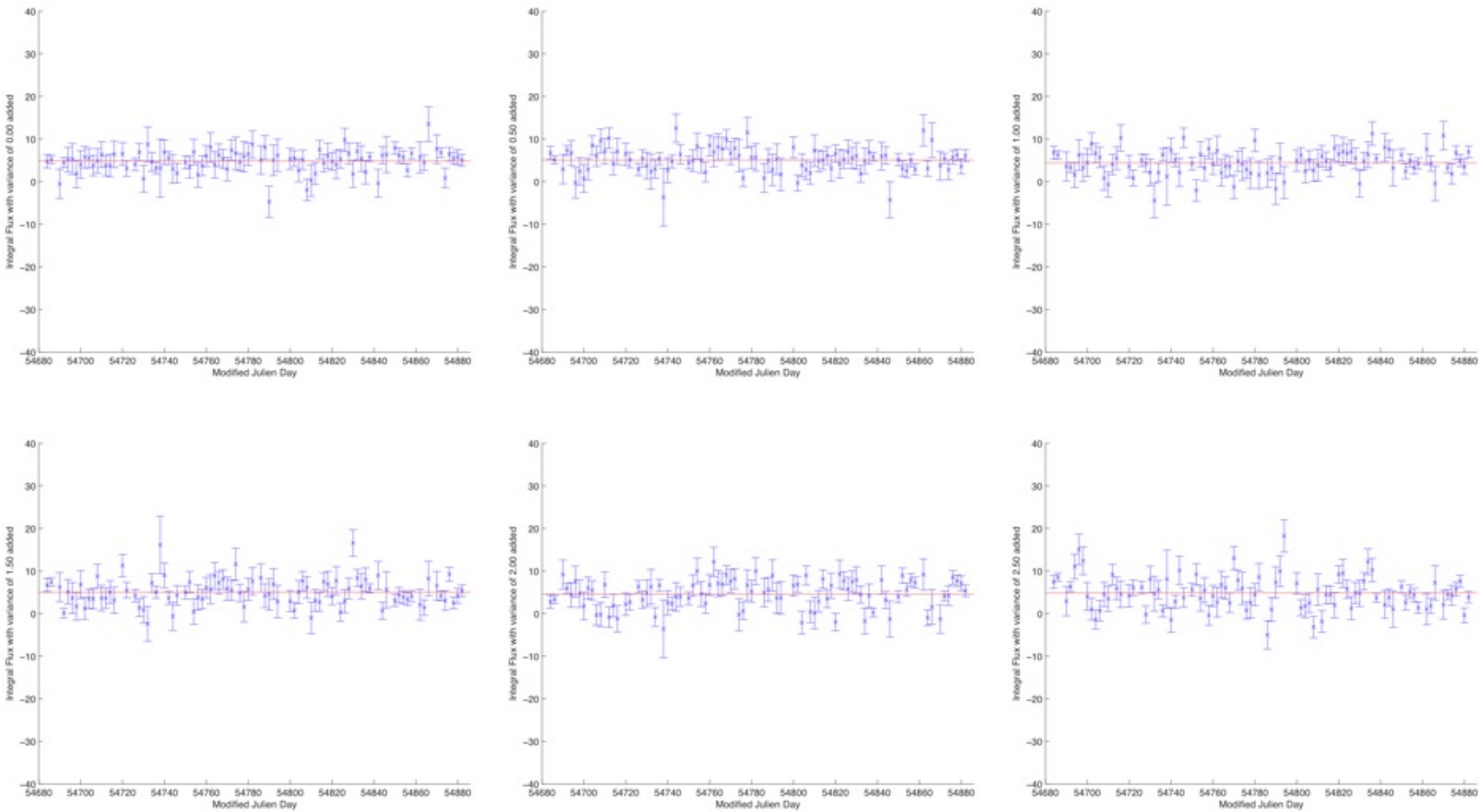

Characterising variability

Putting an upper limit on the excess variance

➡ When no (negative) excess variance is measured in the data, we can estimate the level of intrinsic variance that could be present in the lightcurve but that would still allow us to arrive at this value for excess variance

1. Simulate lightcurves by generating, for each datapoint F_i +/- dF_i (F is the ith data point and dF is the ith uncertainty, i =1:N), a normal distribution centred on the mean of the measured lightcurve with width of sqrt(dF_i^2 + VARIANCE^2)
2. For each level of VARIANCE, generate a large number of lightcurves
3. Calculate the excess variance for each of these lightcurves and histogram these for each level of VARIANCE

Characterising variability

Histograms of excess variance for each VARIANCE added

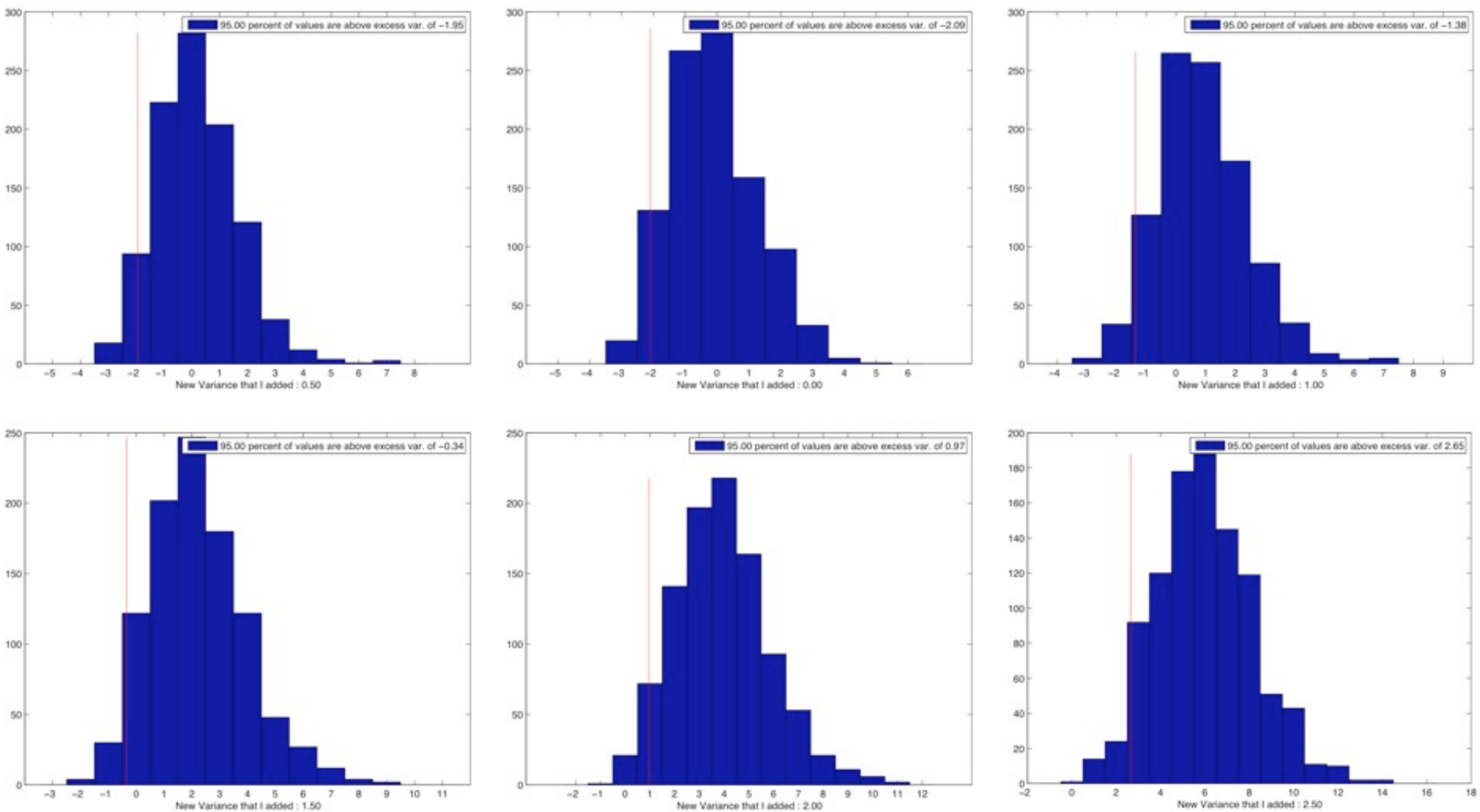

Characterising variability

Putting an upper limit on the excess variance

➡ When no (negative) excess variance is measured in the data, we can estimate the level of intrinsic variance that could be present in the lightcurve but that would still allow us to arrive at this value for excess variance

1. Simulate lightcurves by generating, for each datapoint F_i +/- dF_i (F is the ith data point and dF is the ith uncertainty, i =1:N), a normal distribution centred on the mean of the measured lightcurve with width of sqrt(dF_i^2 + VARIANCE^2)
2. For each level of VARIANCE, generate a large number of lightcurves
3. Calculate the excess variance for each of these lightcurves and histogram these for each level of VARIANCE
4. For each VARIANCE level, find the excess variance that 95% (or whatever your required confidence level is) of the excess variances are above

Characterising variability

Histograms of excess variance for each VARIANCE added

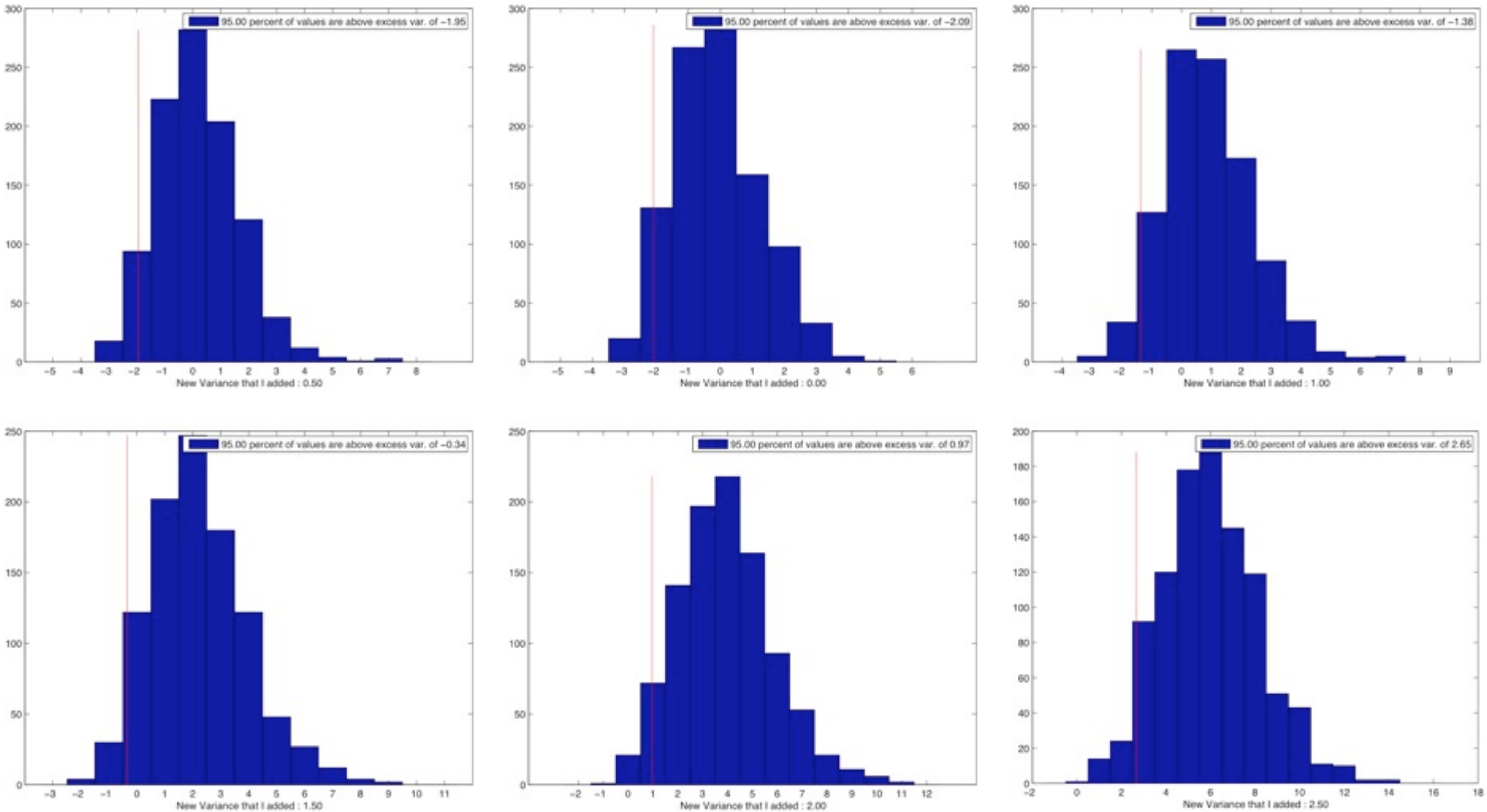

Characterising variability

Putting an upper limit on the excess variance

➡ When no (negative) excess variance is measured in the data, we can estimate the level of intrinsic variance that could be present in the lightcurve but that would still allow us to arrive at this value for excess variance

1. Simulate lightcurves by generating, for each datapoint F_i +/- dF_i (F is the ith data point and dF is the ith uncertainty, i =1:N), a normal distribution centred on the mean of the measured lightcurve with width of sqrt(dF_i^2 + $VARIANCE^2$)
2. For each level of VARIANCE, generate a large number of lightcurves
3. Calculate the excess variance for each of these lightcurves and histogram these for each level of VARIANCE
4. For each VARIANCE level, find the excess variance that 95% (or whatever your required confidence level is) of the excess variances are above

Characterising variability

Putting an upper limit on the excess variance

- By finding where the measured value of excess variance intersects with the curve generated by the 95% values, we can determine the level of VARIANCE that could be present in the lightcurve but that would still lead to us getting the measured value 5% of the time or less

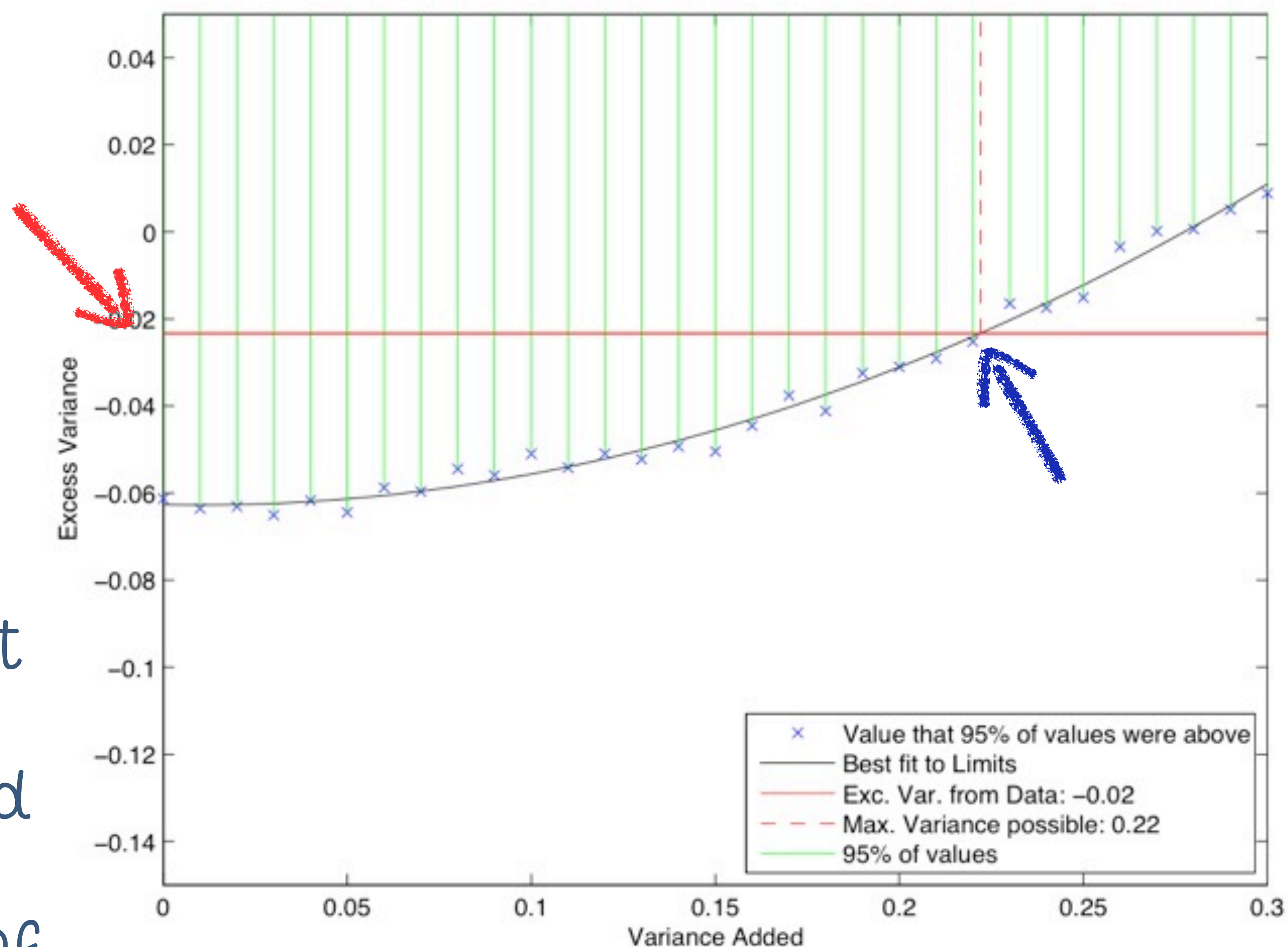

Characterising variability

Note on rate and its uncertainty in Fermi data

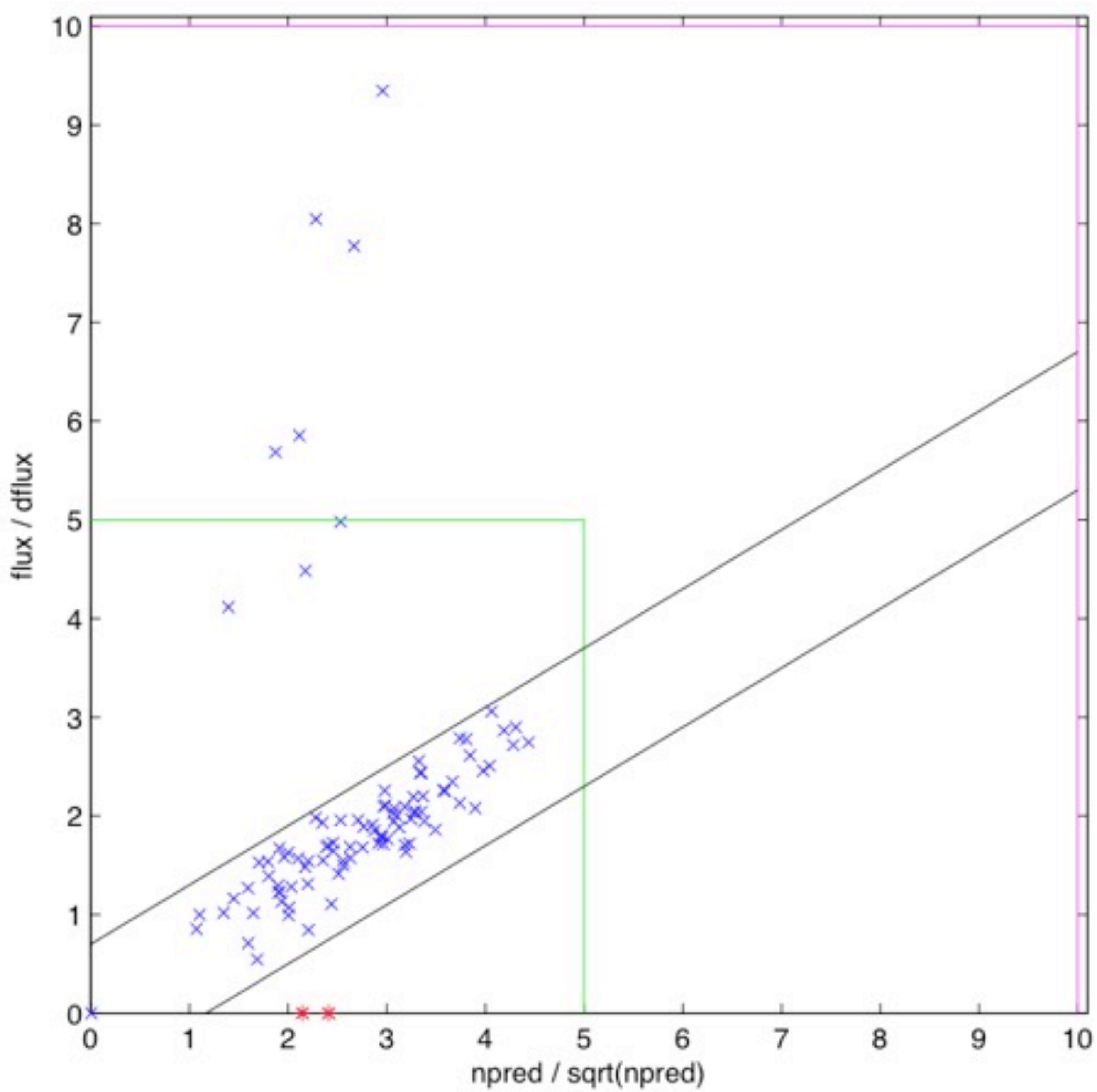

Thank you

for

listening

deirdre@llr.in2p3.fr